

**Argyria F therapy attenuates carcinogenesis of
pancreatic adenocarcinoma (PDAC)**

**Inaugural-Dissertation
zur Erlangung des Doktorgrades
der Medizin**

**der Medizinischen Fakultät
der Eberhard Karls Universität
zu Tübingen**

vorgelegt von

Chen, Xi

2016

Dekan: Professor Dr. I. B. Autenrieth

1. Berichterstatter: Professor Dr. R. R. Plentz

2. Berichterstatter: Professor Dr. P. Seizer

Table of contents

Abbreviations List.....	7
1. Introduction.....	9
1.1 Pancreatic cancer.....	9
1.1.1 Incidence, Mortality and Survival.....	9
1.1.2 Risk Factors.....	10
1.1.2.1 Smoking	10
1.1.2.2 Diabetes.....	11
1.1.2.3 Obesity.....	11
1.1.2.4 Pancreatitis.....	11
1.1.2.5 Other factors.....	12
1.1.3 Symptoms and Diagnosis of PDAC.....	12
1.1.4 Treatments of PDAC	13
1.1.5 Carcinogenesis of PDAC.....	13
1.2 p27kip1 Gene.....	16
1.3 Argyrin F (AF).....	18
1.4 Aims of study.....	18
1.4.1 Work Program.....	18
2. Material and Methods.....	19
2.1 Materials.....	19
2.1.1 Expendable items.....	19
2.1.2 Equipments.....	20
2.1.3 Software.....	22
2.1.4 Chemicals.....	22
2.1.5 Buffers and solutions.....	24
2.1.5.1 Buffers for the cell culture.....	24
2.1.5.2 Buffers and solutions for protein extraction and analysis..	25
2.1.5.2.1 Protein extraction.....	25

2.1.5.2.2 Protein analysis.....	27
2.1.6 Antibodies.....	29
2.1.6.1 Antibody for Western blot.....	29
2.1.6.2 Solutions and antibodies for immunohistochemistry.....	30
2.1.6.3 Primers and PCR program for Genotyping.....	31
2.1.6.3.1 Primers.....	31
2.1.6.3.2 PCR program.....	31
2.2 Methods.....	34
2.2.1 Cells Culture.....	34
2.2.1.1 Cell lines and culture medium.....	34
2.2.1.2 Subculturing adherent cell lines.....	34
2.2.1.3 Quantification of cell number and viability with hemocytometer and trypan blue staining.....	35
2.2.1.4 Preservation of cell lines.....	35
2.2.1.4.1 Freezing.....	35
2.2.1.4.2 Thawing.....	35
2.2.2 Drug preparation and in vitro treatment.....	36
2.2.2.1 Agyrin F.....	36
2.2.2.2 In vitro Treatment	36
2.2.3 Determination of cell number and proliferation using WST-1 assay.....	36
2.2.4 Apoptosis Assays.....	37
2.2.4.1 Annexin V + Propidium iodide (PI) apoptosis assay.....	37
2.2.4.2 Experimental Procedure.....	38
2.2.5 Migration analysis with Wound-healing assay.....	39
2.2.5.1 Migration process.....	39
2.2.5.2 Experimental Procedure.....	39
2.2.6 Invasion measurement with BD Matrigel™ Invasion	

Chamber BioCoat™	40
2.2.6.1 BD Matrigel Invasion Chamber BioCoat.....	40
2.2.6.2 Experimental Procedure.....	40
2.2.7 Soft Agar Assay.....	41
2.2.7.1 Soft agar colony formation.....	41
2.2.7.2 Experiment Procedure.....	42
2.2.8 Protein extraction and western blotting.....	42
2.2.8.1 Cell Culture, -ernte and -lyse.....	42
2.2.8.2 Determination of protein concentration.....	43
2.2.8.3 Production of separating and stacking.....	43
2.2.8.4 Electrophoresis.....	43
2.2.8.5 Protein transfer to PVDF membrane.....	44
2.2.8.6 Antibody incubation and development.....	44
2.2.9 Cell Senesence assay.....	44
2.2.9.1 X-gal.....	44
2.2.9.2 Experiment Procedure.....	45
2.2.10 Cell Cycle.....	45
2.2.10.1 Cell-cycle analysis.....	45
2.2.10.2 Experiment Procedure.....	47
2.2.11 Animals and treatment.....	47
2.2.11.1 Animals and genotyping analysis.....	47
2.2.11.2 Drug and treatment <i>in vivo</i>	47
2.2.12 Immunohistochemistry.....	48
2.2.12.1 The principle of immunohistochemistry.....	48
2.2.12.2 Experimental Procedure.....	48
2.2.13 Statistical Analyses.....	50
3. Results.....	51

3.1 Argyrin F (AF) treatment inhibits proliferation, migration, invasion and colony formation of human PDAC cell lines	51
3.2 Argyrin F(AF) treatment induces considerable apoptosis compared to senescence in human PDAC cell lines.....	62
3.3 Argyrin F (AF) treatment partially impairs epithelial-mesenchymal transition (EMT) in human PDAC cell lines.....	65
3.4 The effect of AF treatment on p27kip1 and p21waf1/cip1 and on cell cycle distribution in human PDAC cell lines.....	67
3.5 Both AF single and combinational (A+G) treatment inhibit tumor growth and prolong overall survival in KPC mice.....	72
3.5.1 Survival experiment (tumor volume, body weight).....	72
3.5.2 Analysis of metastasis incidence and tumor progression in vivo.....	75
3.5.3 Analysis of Ki-67 and CD34 expression in in vivo PDAC tumors.....	77
4. Discussion.....	81
5. Summary.....	88
6. Zusammenfassung	89
7. References List	90
8. Declaration.....	96
9. List of Publications.....	97
10. Acknowledgments	98
11. Curriculum Vitae	99

Abbreviations List

ABC	avidin-biotin-complex
AF	argyria F
CA19-9	carbohydrate antigen 19-9
Cdk	cyclin dependent kinase
CEA	carcinoembryonic antigen
CP	chronic pancreatitis
CT	computer tomography
DAB	diaminobenzidine
DM	diabetes mellitus
DMSO	dimethylsulfoxid
EMT	epithelial-mesenchymal-transition
EUS	endoscopic ultrasonography
FCS	fetal calf serum
G	gemcitabine
GTP	guanosine-5'-triphosphate
IPMN	intraductal papillary mucinous neoplasm
MCN	mucinous cystic neoplasm
MDCT	multi-detector row computed tomography
MRCP	magnetic resonance cholangiopancreatography
MRI	magnetic resonance imaging

MVD	microvascular density
NF-κB	nuclear factor κB
PanIN	pancreatic intraepithelial neoplasia
PCR	polymerase chain reaction
PDAC	pancreatic ductal adenocarcinoma
PDS	programmed cell death
PI	propidium iodide
PS	phosphatidylserine
RT	room temperature
RTOG	radiation therapy oncology group
SD	standard deviations
UK	united kingdom
US	united states
vs	versus
WST	watersoluble tetrazolium
5-FU	5-fluorouracil

1. Introduction

1.1 Pancreatic cancer

Pancreatic ductal adenocarcinoma (PDAC) is the most (95%) common pancreatic neoplasia. PDAC is a very deadly disease that is characterized by late diagnosis with high incidence of metastases and therefore limited treatment options [1].

1.1.1 Incidence, Mortality and Survival

The incidence rate of PDAC varies between different countries due to variable risk factors like lifestyle factors, such as diet, or environmental factors. There are more male patients diagnosed with PDAC compared to female (Figure.1) [1]. The incidence of PDAC is constantly rising, especially in North America [2], Europe and Japan [3] as well as in China. In the United States (US), PDAC represents the fourth and in Europe the fifth most frequent cause of death from cancer [4]. In 2008, an estimated incidence of PDAC in the US was 37,700 and 279,000 worldwide (Cancer Research UK, 2011). In China, the estimated number of newly diagnosed PDAC cases and deaths were 80,344 and 72,723 in 2011, respectively [5]. The overall five-year survival rate of PDAC patients is less than five percent [6]. At the time of diagnosis, only 10-20% of patients have resectable PDAC [7]. In the US the median age at diagnosis of PDAC is 72 years and, rates are strongly age-dependent. Only about 5-10% of patients develop PDAC before the age of 50 years [1]. Median survival rate of the patients after the surgery ranges from 13 to 21 months and for patients without surgery, the median survival is between 2.5-8 months. Recently, a group from the US showed that patients with high risk of early mortality after surgical resection of PDAC can be identified using simple baseline clinical and

laboratory parameters. Future studies should address preoperative interventions in these patients at high risk of early mortality [8].

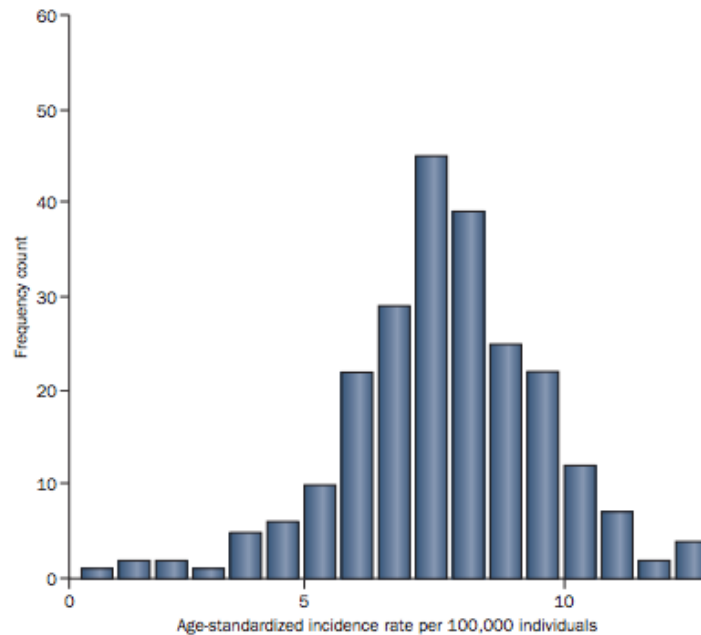


Figure.1 Global age-standardized incidence rates of PDAC in men

Data from the International Agency for Research on Cancer based on countries with >100 PDACs [1].

1.1.2 Risk Factors

Only a few demographic, environmental risk factors and a few genetic autosomal dominant disorders are known to be associated with PDAC. The further risk factors associated with PDAC development are as follows:

1.1.2.1 Smoking

Schulte et al. [9] reported that both smoking intensity and smoking duration were found to be associated with increased risk of PDAC, but smoking intensity is less important than duration or time since quitting. One

meta-analysis showed evidence of non-linear association between smoking intensity and PDAC risk, might differ between sexes [10]. Some mitotic regulator genes might be the potential molecular mediator behind smoking-associated PDAC [11].

1.2.1.2 Diabetes

Diabetes is another risk factor for PDAC development. Tumorigenesis of PDAC and the pathophysiology of type II diabetes mellitus (DM2) are emerging as intertwined pathways. DM2 suggests pancreatic dysfunction and possible an early risk factor for PDAC [12]. Patients with type I diabetes (DM1) or early onset of diabetes have a double risk for PDAC development [13]. Furthermore, Austin et al. reported that also family history of diabetes was associated with increased risk of PDAC [14].

1.2.1.3 Obesity

A meta-analysis of 6391 patients with PDAC found a relative risk of 1.19 for cancer among obese persons, compared with persons of normal weight [15]. The available data for obesity are convincing, and reinforce the concept that maintaining a healthy body weight can prevent PDAC.

1.2.1.4 Pancreatitis

Another known risk factor is pancreatitis, especially chronic pancreatitis [16]. A recent meta-analysis including 22 studies found an increased relative risk of developing PDAC of 5.1 in patients with unspecified pancreatitis, 13.3 in patients with chronic pancreatitis and 69 for hereditary pancreatitis with a lifetime risk of 40–55% [17].

1.2.1.5 Other factors

Other risk factors include family history, advancing age, male gender, non-O blood group, occupational exposures (eg, to chlorinated hydrocarbon solvents and nickel), African-American ethnic origin, and possibly *Helicobacter pylori* infection and periodontal disease [1]; [18];[19];[20].

1.1.3 Symptoms and Diagnosis of PDAC

PDAC is generally known as a clinical silent disease in its early stages. It often grows and metastasizes without significant symptoms which make it difficult for early diagnose. Clinically, the main symptoms of PDAC include indigestion, nausea, weight loss, jaundice, steatorrhea, abdominal and/or back pain. However, patients with PDAC are often asymptomatic. Jaundice and abdominal pain may occur in the progressive stage of PDAC, whereas some nonspecific symptoms, such as indigestion and weight loss, are easily mistaken for other diseases. Regarding this situation, the majorities of patients have the median tumor size about 3.1 cm at the time of diagnosis and thus reduces the chances of curative surgical resection of the tumors [21]. Although initial diagnosis become more important for the patients, but still it remains to be one of the greatest challenges in the fight against cancer in the 21st century. Now available pancreatic imaging has a key role in the characterization of pancreatic focal lesions, initial staging, surgical plan, and assessment of the treatment response using various imaging modalities, including computer Tomography (CT), endoscopic ultrasonography (EUS), Magnetic Resonance Imaging (MRI) and Magnetic resonance cholangiopancreatography (MRCP), et al. [22]. Meanwhile MRI is commonly used to detect PDAC when a mass lesion is not identifiable by CT scan or MRCP [23]. One of the serological markers for diagnosis and monitoring of therapy is the tumor marker

carbohydrate antigen 19-9 (CA19-9). Carcinoembryonic antigen (CEA) is another known marker for diagnosis and monitoring of PDAC [24].

1.1.4 Treatments of PDAC

Surgical resection offers hope for curative therapy of PDAC, but only 20% of patients present with potentially resectable tumors [25];[26]. Even with surgical resection, 5-year survival rates remain dismal, at approximately 20% following the surgery [25]. Due to its poor detection rate, 60%-70% of patients present with metastatic PDAC upon initial diagnosis. Chemotherapy is the main therapy for the advanced disease. Gemcitabine monotherapy became a standard first-line treatment option for metastatic pancreatic cancer after it demonstrated superior clinical benefit over 5-fluorouracil [27]. It has been shown to prolong the average survival rate by 4 months. Renouf et al. [28] reported a phase II study of erlotinib in patients with advanced pancreatic cancer previously treated with gemcitabine, median survival was 3.8 months and 6 month overall survival rate was 32%. Conroy et al. reported that the median overall survival was 11.1 months in the FOLFIRINOX group as compared with 6.8 months in the gemcitabine group. Median progression-free survival was 6.4 months in the FOLFIRINOX group and 3.3 months in the gemcitabine group [7]. Goldstein, et al. [29] reported the median overall survival was statistically significantly longer for nab-paclitaxel plus gemcitabine vs. gemcitabine alone (8.7 vs 6.6 months) for metastatic PDAC patients. In general, systemic chemotherapy in PDAC is still limited.

1.1.5 Carcinogenesis of PDAC

The classical and well-characterized precursor lesions of PDAC show a ductal phenotype, suggesting a ductal cell of origin of this tumor. A major advance in the pathological assessment has been in agreement that pancreatic

intraepithelial neoplasia (PanIN), mucinous cystic neoplasm [8], and intraductal papillary mucinous neoplasm (IPMN) are different precursor lesions for PDA (Figure.2).

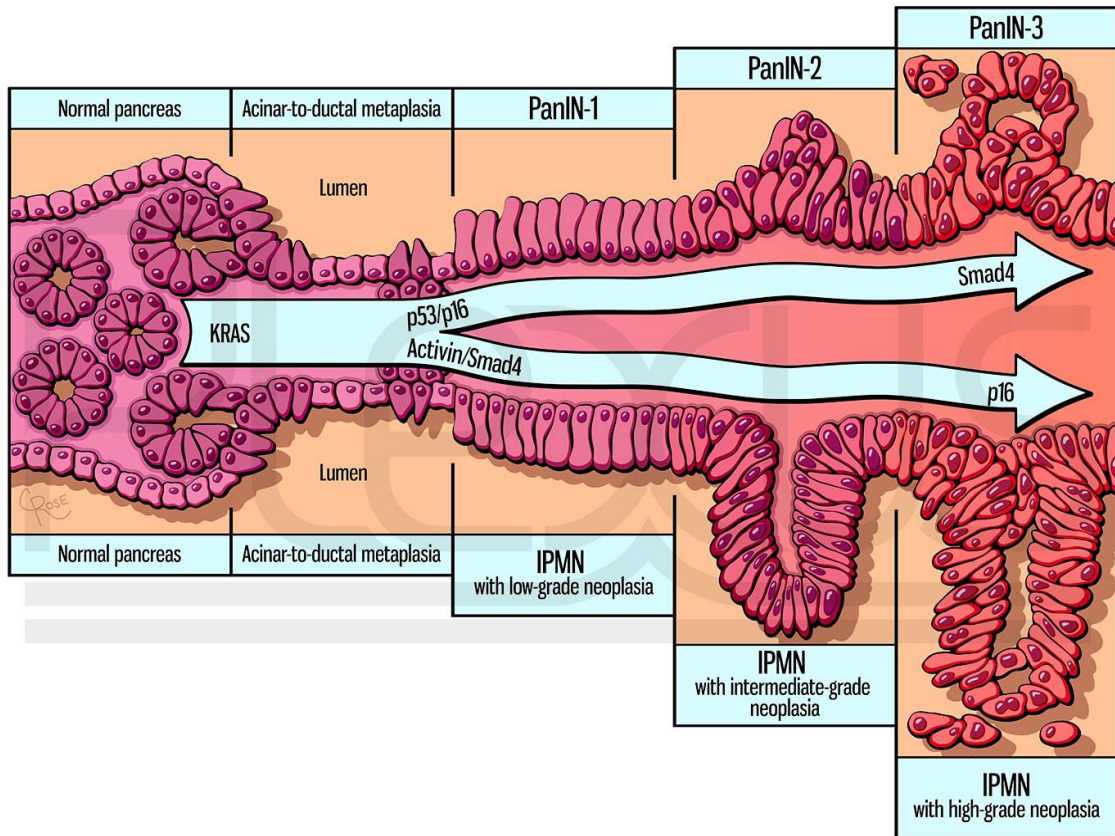


Figure.2 Pathways of PDAC progression

These alternate versions of the same medical illustration were created to highlight the divergent paths that ductal and acinar cells undergo when developing into the pancreatic ductal adenocarcinoma precursors PanIN and IPMN [31].

In 2003, the first transgenic mouse model that faithfully recapitulates the development of PDAC from low-grade precursors to metastatic cancer has been generated [32]. PanIN lesions, are classified as PanIN1a, PanIN1b, PanIN2, and PanIN3 which are allied with progressive alterations in the nuclei, epithelial polarity and architecture, and end in carcinoma *in situ* state (PanIN3) [33]. It has been shown that virtually all PanINs, including more than 90% of

low-grade PanINs, harbor mutations in the Kras gene locus, followed by CDKN2A/p16, SMAD4 and Tp53 mutations in intermediate and later stages of pancreatic carcinogenesis [34]; [35]; [36]. Kras is a Guanosine-5'-triphosphate (GTP) -binding protein and belongs to the member of the Ras family that facilitates a diversity of cellular functions like proliferation, differentiation, and survival [37]. The mutation of oncogene Kras can be detected almost 100% in advanced PDAC [38]. In another study, mutant Kras in acinar cells resulted in neoplastic lesions in mouse pancreas that progressed to PDAC in conjunction with Tp53 deletion [39]. Nuclear factor κ B (NF- κ B) is known to play a key role in inflammation is the transcription factor and its activity has also been observed in PDAC tissue. In addition to Kras mutations, many genetic mutations are reported in PDAC. Biankin et al [16] performed exome sequencing and copy number analysis in a cohort of 142 sporadic PDAC cases and reported multiple significantly mutated genes, including the known mutations- Kras, Tp53, CdkN2A, SMAD4, MLL3, TGFBR2, ARID1A, SF3B1 and some gene also play an important role in PanIN progression. Abrogation of CdkN2A can occur in low-grade or early stage of PanIN, whereas aberrations of Tp53 and SMAD4 can be detected in high-grade/late PanINs [40]. It is increasingly understood that PDAC consist microenvironment composed of dense fibrotic stroma with cancer cells, stellate cells, infiltrating inflammatory cells, fibroblasts which are responsible for the production of collagen and fibronectin [41]. The tumors also consist of cancer stem cells which are thought to be responsible for chemotherapy resistance.

Epithelial-to-mesenchymal transition (EMT) is the progression that makes the conversion of adherent epithelial cells into independent fibroblastic cells possessing migratory properties and the ability to invade the extracellular

matrix [42]; [43]. *In vitro*, various carcinoma cell lines undergo partial or complete EMT (Figure.3). Beuran, et al. [44] concluded that there is a strong correlation between the EMT and the systemic aggressiveness of PDACs. Consequences of the EMT are the loss epithelial marker (E-cadherin) expression and the acquisition of mesenchymal markers including N-cadherin or Vimentin. Molecular processes underlying the EMT have opened possibilities for new therapeutic agents.

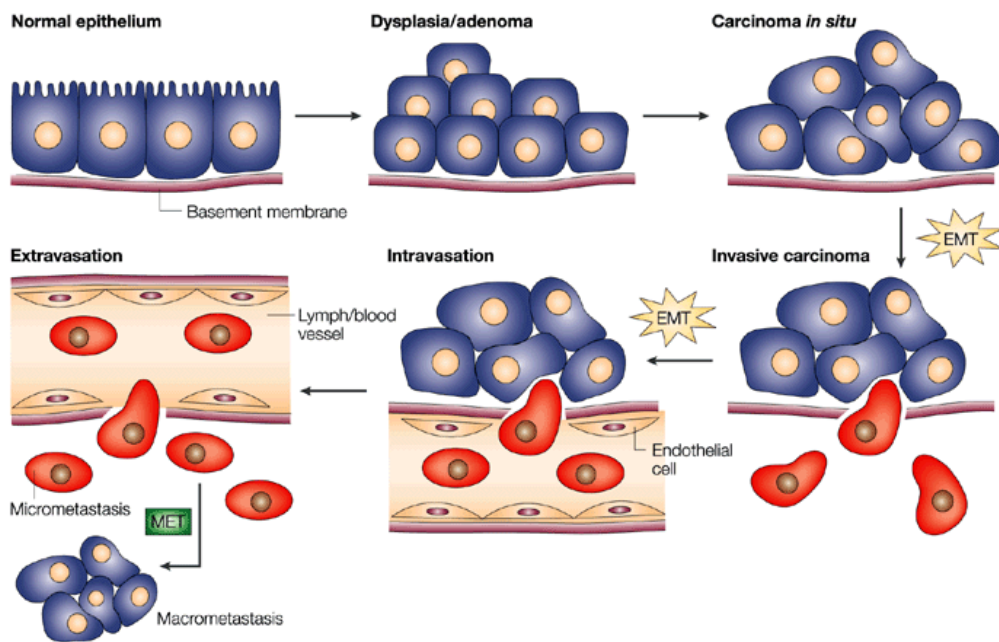


Figure.3 Sites of EMT in the emergence and progression of carcinoma

Normal epithelia lined by a basement membrane can proliferate locally to give rise to an adenoma. Further alterations can induce local dissemination of carcinoma cells, possibly through an epithelial-mesenchymal transition (EMT).

1.2 p27^{Kip1} Gene

Cyclin-dependent kinase inhibitor 1B (p27^{Kip1}) is an enzyme inhibitor that in humans is encoded by the CdkN1B gene [45]. p27^{Kip1} belongs to the “Cip/Kip” family of cyclin dependent kinase (Cdk) inhibitor proteins. p27^{Kip1} binds to and prevents the activation of cyclin E-Cdk2 or cyclinD-Cdk4 complexes, and thus controls the cell

cycle progression at G₁ phase. It is often referred as a cell cycle inhibitor protein. The p27^{Kip1} gene has a DNA sequence similar to other members of the "Cip/Kip" family which include the p21^{Cip1/Waf1}. p27^{Kip1} is considered a tumor suppressor because of its function as a regulator of the cell cycle (Figure. 4). p27^{Kip1} can inhibit or promote cell motility, data increasingly indicate that p27^{Kip1} integrates mechanisms regulating cell proliferation, migration, invasion and metastasis.

The Loss of expression or down regulation of p27^{Kip1} protein can be observed in many cancers and is proved to be an independent prognostic factor in these malignancies [46]. Juuti et al. showed that loss of p27^{Kip1} expression was associated with poor prognosis in stage I-II of PDAC; the 5-year survival for p27^{Kip1} negative patients was 3.6% compared with 20% for p27^{Kip1}-positive patients (p= 0.03) [47]; [48].

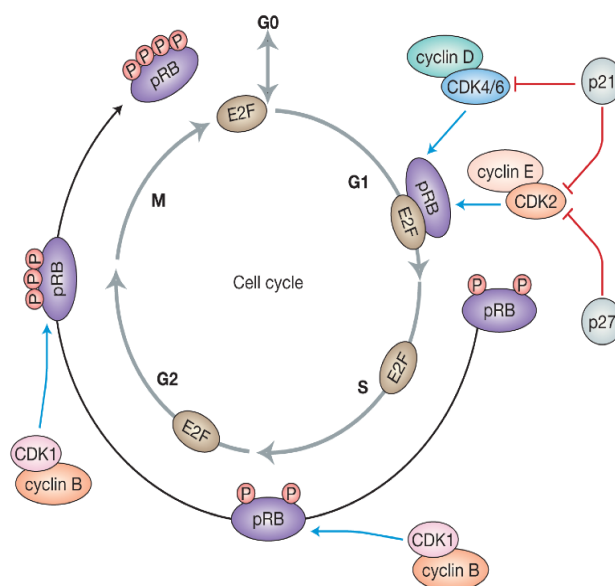


Figure.4 Cell cycle progression is regulated by cyclin–Cdk complexes

Schematic diagram shows different classes of Cyclin and Cdk molecules. p27^{Kip1} inhibits the catalytic activity of Cyclin E/Cdk2 as well as Cdk4. Increased the level of p27^{Kip1} can cause cell to rest in G₁ phase of the cell cycle [49] ;[50].

1.3 Argyrin F (AF)

Nickeleit, et al. [51] identified Argyrin A as a proteasome inhibitor that by preventing the destruction of the cyclin kinase inhibitor p27^{kip1} exerts broad antitumoral activities. All antitumoral activities of Argyrin A depend on the prevention of p27^{kip1} destruction, as loss of p27^{kip1} expression confers resistance to this compound. Argyrin A has several analogues and AF is one of them, it is a chemically synthesized cyclical peptide with potent antitumoral activity [52]. Bülow, et al. have tested AF on colon cell lines and find that AF treatment resulted in an up-regulation of p27^{kip1} in SW-480 colon carcinoma cells in a dose-dependent manner like Argyrin A, requiring p27^{kip1} expression for the induction of its biological phenotype [52]. They found that AF leads to an even faster destruction of blood vessels *in vivo* compared to Argyrin A which increases the ability of AF to reduce the size of solid tumors in mice models [52]. Based on these studies, we set out to identify the antitumor effect of AF on PDAC.

1.4 Aims of study

The major aim of the present study is to explore the anti-tumor activity of Argyrin F against PDAC.

1.4.1 Work Program

- Analysis of cell proliferation and apoptosis under AF treatment
- Analysis of cell colony formation under AF treatment
- Analysis of migration and invasion under AF treatment
- Analysis of cell senescence under AF treatment
- Analysis of EMT under AF treatment
- Analysis of cell cycle under AF treatment
- *In vivo* therapy of AF and AF+Gemcitabine (G) treatment in a PDAC mouse model: analysis of survival, tumor volume, cell proliferation and angiogenesis

2. Material and Methods

2.1 Material

2.1.1 Expendable items

Cover slip	Menzel-Glaeser, Braunschweig
Freezing tube	Sarstedt, Nürnberg
Microscope slides	Menzel-Glaeser, Braunschweig
Transfer membrane	Perkin Elmer, Rodgau
Hyperfilm TM ECL	Amersham Bioscience, Braunschweig
Whatman	Omnilab, Elbingeröder
Centrifuge tubes	Beckmann, Palo Alto
Dialysis tubing	Pierce, Rockford
6 wells plate	Sarstedt, Nürnberg
12 wells plate	Sarstedt, Nürnberg
96 wells plate	Sarstedt, Nürnberg
Cell culture dishes 1000x15 mm	Sarstedt, Nürnberg
Cell culture dishes 60x15 mm	Greiner Bio-One, Frickenhausen
Micro tube 1,5 ml	Sarstedt, Nürnberg
Filter Tips 0,1-10 ul	Sarstedt, Nürnberg
Filter tips 20 ul	Sarstedt, Nürnberg
Filter tips 200 ul	Sarstedt, Nürnberg
Filter tips 1000 ul	Greiner, Solingen
15 ml tube	Sarstedt, Nürnberg
50 ml tube	Sarstedt, Nürnberg

2.1.2 Equipments

Agarose Gelelectrophoresis systems	Bio-RAD, München
Centrifuges:	Eppendorf, Hamburg
Centrifuge 5415 D	Roth Karlsruhe
Centrifuge Mikro 220 R cooled	Heraeus, Osterode
Megafuge 1.0	Hettich, Tuttlingen
Centrifuge "Rotina 38R"	Beckman GmbH, Düsseldorf
Centrifuge "L8-55M"	GFL, Burgwedel
Chaker vibramax 110	Heidolph, Kelheim
Clean Bench	Hera Safe, Kendro, Osterode
Easypet 4420	Sartorius, Göttingen
Electrophoresis power supply	Leica DM5000, Leica, Wetzlar
Fluorescence microscope	Bio-RAD, München
Gel chambers for proteins	Bio-RAD, München
Heater	Heraeus, Instruments GmbH, Osterode
Incubator	Heidolph, Kelheim
Magnetic stirrers	Bio-RAD, München
MicroPulser™	Tecan Deutschland GmbH, Crailsheim
Microtiterplate luminometer	Bauknecht, Stuttgart
Microwave	Bio-RAD, München
Mini-Protein Electrophoresis System	Bio-RAD, München
Mini Trans-Blot cell	Bio-RAD, München
Mixer 5432	Eppendorf, Hamburg
Multipette® plus	InoLab, Weilheim
pH-meter	Eppendorf, Hamburg
Photometer	Eppendorf, Hamburg
Pipett	Hirschmann, Eberstadt
Pipetman	Bio-RAD, München

Power supplies	Gilson, Villiers le Bel
Sonifier UP 200H	Bio-RAD, München
Thermo cycler	Hielscher, Stahnsdorf
Thermomixer 5436	MWG-Biotech AG, Ebersberg
ThermoStat plus	Eppendorf, Hamburg
Vortex-Genie	Eppendorf, Hamburg
Water baths	Janke & Kunkel, Staufen

2.1.3 Software

Microsoft Excel 2007 (Microsoft Inc., Remond, Washington, USA)
Microsoft Word 2007 (Microsoft Inc., Remond, Washington, USA)
FlowJo Version 7.3 (Tree Star Inc., Ashland, USA)
BD Cell Quest Pro™ (BD Biosciences, Mississauga, USA)
ImageJ 1.42 (Free Software Foundation, Inc., Boston, USA)
Adobe Photoshop 7.0 (Adobe Systems, San Jose, USA)
MacVector Version 10.1 (MacVector Inc, Cambridge, UK)

2.1.4 Chemicals

Acetic acid	Baker, Griesheim
Aceton	Merck, Darmstadt
Acrylamid-solution (30%) Mi 37,5:1	AppliChem, Darmstadt
Annexin V conjugates	AppliChem, Darmstadt
Agar	Bioline, Luckenwalde
Agarose	Bioline, Luckenwalde
Argyrin F	Leibniz Universität Hannover
Ammoniumacetat	AppliChem, Darmstadt
Ammoniumsulfat	AppliChem, Darmstadt

Ampicillin	Vector, Eching
Antigen unmasking solution	Sigma-Aldrich, Schnelldorf
Antifoam	Becton Dickinson, Heidelberg
Bacto™ peptone	Sigma-Aldrich, Schnelldorf
Benzamidine	Roche, Mannheim
β-Glycerophosphat	AppliChem, Darmstadt
β-Mercaptoethanol	AppliChem, Darmstadt
Bromophenol bleu	AppliChem, Darmstadt
Boric acid	Merck, Darmstadt
Calcium chlorid	AppliChem, Darmstadt
Cesium chloride 99%	AppliChem, Darmstadt
DAB substrate Kit	Vector, Eching
DEPC	AppliChem, Darmstadt
dNTP	Fermentas, St. Leon-Rot
EDTA	AppliChem, Darmstadt
EGTA	AppliChem, Darmstadt
Ethanol	Meck, Darmstadt
Ethanolamine	Sigma-Aldrich, Schnelldorf
Ethidiumbromide	AppliChem, Darmstadt
FCS	Biochrom, Berlin
Formaldehyde solution min. 37% free from acid	Merck, Darmstadt
Gelatine	Sigma-Aldrich, Schnelldorf
Glucose	AppliChem, Darmstadt
GlutaMax	Invitrogen, Karlsruhe
Glycine	AppliChem, Darmstadt
G-sepharose beads	GE Healthcare, München
Guanidine thiocyanate	Sigma-Aldrich, Schnelldorf

HEPS	AppliChem, Darmstadt
30% H ₂ O ₂	Sigma-Aldrich, Schnelldorf
Hot start DNA Polymerase	Qiagen, Hilden
Imidazole	AppliChem, Darmstadt
Isopropanol	Merck, Darmstadt
Kanamycinesulfate	AppliChem, Darmstadt
Lauroylsarcosine	Sigma-Aldrich, Schnelldorf
Luminol min 97%, HPLC	Sigma-Aldrich, Schnelldorf
Magnesium chloride	AppliChem, Darmstadt
Methanol	AppliChem, Darmstadt
MG132	Sigma-Aldrich, Schnelldorf
Mounting Medium	Vector, Eching
MTT assay WST-1	Roche, Mannheim
Natrium	AppliChem, Darmstadt
Natriumchlorid	AppliChem, Darmstadt
Noble Agar	BD Difico, Heidelberg
Nonfat dried milk powder	AppliChem, Darmstadt
Nonidet P40	AppliChem, Darmstadt
Normal Horse Serum	Vector, Eching
p- Cumaric acid	Merck-Schuchard, Darmstadt
Penicillin-Streptomycin solution	Invitrogen, Karlsruhe
Phenol	AppliChem, Darmstadt
Polyethylenimine	PfuTurbo DNA polymerase
Ponceau S solution	Roth, Karlsruhe
Potassium acetate	Sigma-Aldrich, Schnelldorf
Potassium chlorid	AppliChem, Darmstadt
Potassium dihydrogen	AppliChem, Darmstadt
phosphate	AppliChem, Darmstadt

Prolong® gold antifade reagent	Merck, Darmstadt
Propidium iodid	Invitrogen, Karlsruhe
Proteinase K	Fluka, Steinheim
Restriction enzymes	AppliChem, Darmstadt
SDS	NEB, Fermentas
Sodium carbonate	AppliChem, Darmstadt
Sodium chloride	AppliChem, Darmstadt
Sodiumdihydrogenphosphat	AppliChem, Darmstadt
Sodium floride	AppliChem, Darmstadt
Sodium pyrophosphate	AppliChem, Darmstadt
Talon metal affinity resins	Sigma-Aldrich, Schnelldorf
TEMED	Becton Dickinson, Heidelberg
Thymidine 99-100%	AppliChem, Darmstadt
Thermo Pol buffer	Sigma-Aldrich, Schnelldorf
Tris	Biolabs, Frankfurt
Triton X 100	AppliChem, Darmstadt
Trypsin/EDTA solution	AppliChem, Darmstadt
Trypton	Biochrom, Berlin
Tunicamycin	AppliChem, Darmstadt
Tween-20	Sigma-Aldrich, Schnelldorf
Urea	AppliChem, Darmstadt
Vectastain Elite	AppliChem, Darmstadt
ABC-Peroxidase Kits	Vector, Eching
X-Gal for microbiology BC	Peqlab, Erlangen
Xylenecyanol	AppliChem, Darmstadt

2.1.5 Buffers and solutions

2.1.5.1 Buffers for the cell culture

Dialysis buffer pH 7,4

HEPS	10 mM
NaCl	150 mM

10X PBS

NaCl	137 mM
KCL	2,7 mM
Na ₂ HPO ₄	100 mM
KH ₂ PO ₄	2 mM

The pH was adjusted to 7,4. PBS was sterilised by autoclaving.

Annexin-binding buffer pH 7,4

HEPS	10 mM
NaCl	140 mM
CaCl ₂	2,5 mM

Proteinase K buffer

Tris pH 8,5	100 mM
EDTA	5 mM
SDS	0,2 %
NaCL	200 mM
ddH ₂ O	100 ml

2.1.5.2 Buffers and solutions for protein extraction and analysis

2.1.5.2.1 Protein extraction

RIPA

Tris pH 8,0	50 mM
NaCl	80 mM
NaF	50 mM
Na ₄ P ₂ O ₇	20 mM
EDTA	1 mM
EGTA	1 mM
NP-40	1 %
DOC	1 %
SDS	0,1 %

NP40

Tris pH 7,5	50 mM
NaCl	150 mM
NaF	50 mM
Na ₄ P ₂ O ₇	20 mM
EDTA	1 mM
β Glycerolphosphat	10 mM
NP-40	0, 5 %

4XSB

Tris pH 6,8	0,25 M
SDS	8 %
Glycerol	40 %
β-Mercaptoethanol	10 %
Bromophenol blue	0,05 %

Protease and phosphatase inhibitors (for 10 ml buffer)

	Inhibitor of	Final concentration
Vanadat	Tyrosin-phosphatase	100 uM
Leupeptin	Aspartic-protease	0,5 ng/ml
Leupeptin	Serin-cystein protease	2,5 ng/ml
Benzamidin	Trypsin, thrombin, Plasmin	0,15 mM
Aprotonin	Trypsin, chymotrypsin, Kallikerin	0,5 %
PMSF	Serin-protease	0,5 mM

Table 1: List of the used protease and phosphatase inhibitors

2.1.5.2.2- Protein analysis

Separating Gel

% Acrylamid	7,5 %	10 %	12 %	14 %	15 %
Acrylamid	2,5 ml	4,1 ml	3,4 ml	2,7 ml	2,45 ml
Tris pH 8,0	2,5 ml	2,5 ml	2,5 ml	2,5 ml	2,5 ml
H ₂ O	4,85 ml	4,1 ml	3,4 ml	2,7 ml	2,45 ml
10 % SDS	100 ul	100 ul	100 ul	100 ul	100 ul
TEMED	15 ul	15 ul	15 ul	15 ul	15 ul
10 % APS	105 ul	105 ul	105 ul	105 ul	105 ul

Table 2: Recipes of the used separating gels

Stacking gel

Acrylamid	1,13 ml
Tris 6,8 pH	1,75 ml
ddH ₂ O	3,2 ml

10 % SDS	70 ul
TEMED	7 ul
10 % APS	70 ul

Table 3: Recipe of the used stacking gel

SDS running buffer (10x)

Tris pH 8,3	250 mM
SDS	1 %
Glycine	1,92 M

Western transfer buffer (10x)

Tris	250 mM
Glycine	1,92 M

TNT western blot washing buffer (10x)

NaCL	1,5 M
Tris pH 7,5	100 mM
Tween-20	0,5 %

Blocking solution

Milk powder, nonfat 5 % in TNT

ECL solution

Solution 1

Luminol	250 mM
p-cumaric acid	0,4 mM
Tris pH 8,5	0,1 M

Solution 2

Tris pH 8,5	0,1 M
30 % H ₂ O ₂	0,061 %

2.1.6 Antibodies

2.1.6.1 Antibody for Western blot

Primary antibody

Target	Working dilution	Source	Manufacturer
Anti-E-Cadherin Rabbit mAb	1:1000	rabbit	Cell signaling
Anti-N-cadherin rabbit monoclonal	1:50000	rabbit	Millipore
Polyclonal anti-P21 (C-19)	1:500	rabbit	Santa cruz
Polyclonal anti-P27 (C-19)	1:500	rabbit	Santa cruz
Monoclonal anti-Actin (C-2)	1:10000	mouse	Santa cruz

Table 4: List of primary antibodies used for western blot

Secondary antibodies

Target	Working dilution	Manufacturer
Anti-mouse IgG peroxidase conjugated	1:10000	Amersham, 1,5 mg/ml
Anti-rabbit IgG peroxidase conjugated	1:10000	Amersham, 1,5 mg/ml
Mouse TrueBlot™ HRP-conjugated anti-mouse IgG (clone eB144/7A7)	1:15000	Bioscience

Table 5: List of secondary antibodies used for western blot

2.1.6.2 Solutions and antibodies for immunohistochemistry

Antigen Unmasking Solution

Antigen unmasking solution 1:100 diluted in dH₂O

Blocking Solution (in PBS)

Normal Horse serum 5%

Trinton X-100 0.3%

Acid Rinse Solution

Glacial Acetic acid 2%

Ethonal

100%, 95%, 70%, 40%

Primary antibody

Target	Working dilution	Source	Manufacturer
Ki-67	1:200	mouse	Novocastra
Anti-CD34 antibody	1:200	mouse	Novus

Table 6: List of primary antibodies used for IHC

2.1.6.3 Primers and PCR program for Genotyping

2.1.6.3.1 Primers

p53 forward	AGCACATAGGAGGCAGAGAC	Sigma-Aldrich
p53 backward	CACAAAAACAGGTAAACCCAG	
5`-Kozak-3`LoxP1	CTAGCCACCATGGCTTGAGT	
3`-Flank-5`LoxP1	TCCGAATTCAGTGACTACAGATG	
Gabra 12	CAATGGTAGGCTCACTCTGGGAGATGATA	
Gabra 70	AACACACACTGGCAGGACTGGCTAGG	
Pdx1-Cre 26	CCTGGAAAATGCTTCTGTCCG	
Pdx1-Cre 36	CAGGGTGTTATAAGCAATCCC	

Table 7: List of used primers for genotyping

2.1.6.3.2 PCR program

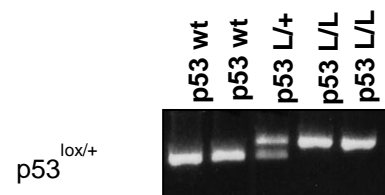
p53^{lox/+}

15,87 µl MilliQ

2 µl 10x ThermoPol Reaction Buffer

0,13 25mM MgCl₂

0,5 µl Primer p53 Forward



0,5 µl Primer p53 Backward
 0,4 µl dNTP's
 0,1 µl Qiagen Hot star Taq polymerase

19,5 µl reaction
 + 0,5 µl DNA

20 µl

LSL-Kras^{G12D}

15,5 µl MilliQ water
 2 µl 10x ThermoPol Reaction Buffer
 0,15 25mM MgCl₂
 0,34 µl 20µM Gabra 70
 0,34 µl 20µM Gabra 12
 0,34 µl 20µM 5`-Kozak-3`LoxP1
 0,34 µl 20µM 3`-Flank-5`LoxP1
 0,4 µl dNTP's
 0,1 µl Qiagen Hot star Taq polymerase

LSL-Kras^{G12D}



19,5 µl reaction
 + 0,5 µl DNA

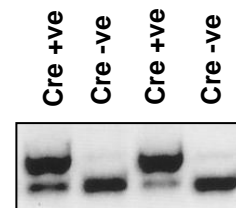
20 µl

---350bp=presence(Kras^{G12D} +) and absence(Kras^{G12D} -)
 bottom band=300bp is internal control (Gabra)

Pdx1-Cre

23,5 µl MilliQ water
 3µl 10x Qiagen Reaction Buffer
 0,2 µl 25mM MgCl₂
 0,5 µl 10µM Gabra 70

Pdx1- Cre



0,5 µl 10µM Gabra 20
 0,5 µl 10µM Cre 36
 0,5 µl 10µM Cre 26
 0,6 µl dNTP's
 0,2 µl Qiagen Hot star Taq polymerase

29,5 µl reaction

+ 0,5 µl DNA

30 µl

---Band 400bp = presence(Pdx1-Cre +) and absence(Pdx1-Cre -)

Bottom band 300bp = internal control (Gabra)

Standard program:

Lid on 110°C

95°C 15' DNA Denaturing

94 °C 30" DNA Denaturing

60 °C 30"-1' Primer Annealing

72 °C 50"-1' Strand Elongation

30 - 33x

72 °C 6' Final Elongation

10 °C Hold

The PCR product can be analysed using agarose gel electrophoresis.

2.2 Methods

2.2.1 Cells Culture

2.2.1.1 Cell lines and culture medium

All operations were performed in a laminar flow hood under aseptic conditions. The work area was always cleaned with 70% ethanol, and sterile cell culture dishes and sterilized glass pipette were used. Cells were regularly tested on mycoplasma contamination. Two human PDAC cell lines: Panc-1 (cultured from a primary tumor without evidence of metastasis) and KP3 (cultured from liver metastases of a human pancreatic tumor) were used in this experiment. Cells were provided by Nabeel Bardeesy (MGH Cancer Center, Boston, USA). These two cell lines were originally obtained from the MGH Center for Molecular Therapeutics (CMT). The cell lines were maintained at 37°C under a 5% CO₂ environment in RPMI 1640+Glutamax (Invitrogen, Karlsruhe, Germany) enriched with 10% fetal calf serum (FCS) (Biochrom, Berlin, Germany) and antibiotics of penicillin / streptomycin (100 units/ml) (Invitrogen, Karlsruhe, Germany). After 2-3 days, the cells were passaged.

2.2.1.2 Subculturing adherent cell lines

Adherent cells were subcultured after reaching 70-90 % confluency. Culture medium was removed from the plate, and cells were washed 2 times with PBS. To detach adherent cells, the plate was incubated with 1 ml trypsin at 37 ° C for 1-2 min. The incubation time might differ from cell line to cell line. . The detached cells can be examined under the microscope and the proteolytic reaction can be quickly terminated by the addition of pre-warmed growth medium. Cells were re-suspended with the appropriate volume of medium and 1x10⁶ cells were split into fresh 10cm² plates containing complete medium. Alternatively, cells can be counted using a hemocytometer and diluted to desired density.

2.2.1.3 Quantification of cell number and viability with hemocytometer and trypan blue staining

To perform accurate quantification and to standardise culture conditions, it is necessary to determine the cell number. The hemocytometer was the instrument used in this work to determine the cell number.

The hemocytometer consists of 4 corner squares, which are divided into 16 tertiary squares. Cells in the four corner squares were counted, and the number of cells per ml was determined according to the following equation:

$$\text{Cells/ml} = \text{average count per square} \times \text{dilution factor} \times 10^4$$

(Each square is 1m^2 and the depth is 0,1 mm)

The number of total cells was counted as follows:

Total cells = cells/ml x the volume of cell suspension from which sample were taken.

2.2.1.4 Preservation of cell lines

2.2.1.4.1 Freezing

For long-term storage cells have to be frozen. FCS was used in combination with 10 % DMSO to store cells at -80°C or lower. The use of DMSO as cryoprotective agent is required to preserve cells, to reduce the freezing point and to allow a slower cooling rate. Gradual freezing is necessary to reduce the risk of ice crystal formation and cell damage. For Freezing, after trypsinisation and centrifugation for 5 min at 800 rpm, the pellet was resuspended in freezing medium to obtain 1×10^6 cells/ml. 1ml aliquots of suspension cells was pipetted into labeled freezing tubes. Covering the tubes with towels allows a slower freezing at -80°C .

2.2.1.5.2 Thawing

Cells were removed from frozen storage and quickly thawed in a 37°C water bath. After thawing, the cell suspension was placed into a 10cm² plate containing 8 ml warm medium. The medium was changed in the next day to remove all traces of DMSO.

2.2.2 Drug preparation and *in vitro* treatment

2.2.2.1 Agyrin F

AF was supplied by Biomolecular drug center (BMWZ), Leibniz University of Hannover. AF was prepared as a 5mg/ml stock in dimethylsulfoxide, DMSO (AppliChem, Darmstadt, Germany) in the Intern medicine I lab, University clinic of Tübingen. Then we make the aliquots of the drug by 0.5mg/ml and keep in -20°C.

2.2.2.2 *In vitro* Treatment

Cells were treated with DMSO or AF in different concentrations (0.5ug/ml, 2ug/ml, 6ug/ml) and were analyzed after 24hrs, 48hrs and 96hrs for certain experiment.

2.2.3 Determination of cell number and proliferation using WST-1 assay

The cell viability was examined by the WST-1 assay (Roche Diagnostics, Mannheim, Germany). Living cells with a functional mitochondrial dehydrogenase will split the red WST-1 (watersoluble tetrazolium) enzymatically. In doing so, it will produce the orange formazan. A total 5x10³ cells with 200 µl complete medium were seeded per well into several sterile 96-well tissue culture plates and PBS was pipetted into the surrounding wells in order to keep the medium from drying. The plates were incubated over night. After 24h incubation in the incubator, one 96 wells cell culture plate was selected as the zero-hour value. In each chamber we put 10 µl WST-1 reagent and after an incubation period of 2 hrs in incubator, The plate were read at a

wavelength of 492 nm with reference wavelength of 650 nm using a Micro plate-Reader Multiskan Plus (Titertek-Berthold, Pforzheim, Germany). Following the treatment with AF in different concentration (0.5ug/ml, 2ug/ml, 6ug/ml) and DMSO control, cells of the remaining plate were further incubated for additional time points (24, 48, 72 and 96 hrs). Every day, cell growth was examined microscopically. Then 10 µl of WST-1 reagent was added per well daily and repeat the same step as zero-hour-value. The averages of proliferations index were obtained during the evaluation on 100% of the untreated control on day zero.

2.2.4 Apoptosis Assays

2.2.4.1 Annexin V + Propidium iodide (PI) apoptosis assay

Apoptosis is the process of programmed cell death (PDS) that may occur in multicellular organisms. The change in the double lipid membrane structure is one of the earliest. In this process, it comes to the translocation of the Membranphospholipids phosphatidylserine (PS) from the inner to the outer membrane, where the membrane remains intact. Annexin V is a protein which has a high binding capacity for PS and thus binds to apoptotic cells. Annexin V may be conjugated to fluorochromes such as FITC and detected by flow cytometry. Since Annexin V but can also bind to PS necrotic cells, simultaneous labeling with PI is carried out, which can pass only in the event of a damaged cell membrane (necrotic or dead cells) in the cell and intercalated in the DNA. Living cells are thus Annexin V and PI negative. Early apoptotic cells are Annexin V positive and PI negative. Late apoptotic cells or dead cells are both Annexin V and PI positive. The quantitative measurement of the percentage of apoptotic cells will be performed in the whole population (according to manufacturer information).

2.2.4.2 Experimental Procedure

Cells were seeded in 6-well tissue culture plates at a density of 1×10^5 cells per well and were incubated over night at 37°C . These cells were further treated with AF as described in proliferation assay. The medium was changed every two days. At 48 and 96 hrs, the cells were harvested. For this purpose, firstly, the spent medium was aspirated and transferred in each case in the corresponding test tube. The cell layer was washed with $1 \times \text{PBS}$ and incubated after addition of 0.5 ml trypsin-EDTA to each well for 60 seconds in an incubator. After the proteolytic, remove of the cells from the medium into the test tubes in the corresponding cavity was transferred back to stop the trypsin activity. Then centrifuge for 5 min at 1000 rpm. The supernatant was discarded, the cell pellet was resuspended with 1 ml $1 \times \text{PBS}$ and centrifuged for another 5 min. The supernatant was discarded again, the cell pellet was suspended with 1ml $1 \times \text{Binding Buffer}$ (FITC Annexin V Apoptosis Detection Kit I, BD Biosciences) on ice. The untreated control was divided into three tubes (Annexin V-control, PI-control and unlabeled control). $5 \mu\text{l}$ Annexin V and $10 \mu\text{l}$ PI (Annexin V FITC Apoptosis Detection Kit I, BD Biosciences) were added into their corresponding tubes. After a fifteen-twenty-minute incubation on ice in dark, the prepared sample should be detected on the flow cytometer within one hour. The signal was detected using FACS calibur flow cytometer (BD, Heidelberg, Germany) and analyzed using FlowJo Version 7.6 software (Tree Star Inc., Ashland, USA). The unmarked population was served as the basal rate of apoptotic cells. The coordinate field has been divided by a cross so that the rate of apoptotic and dead cells of the unlabeled control corresponded to approximately zero. Characterized the proportion of apoptotic cells in the untreated cell population of the other populations of apoptotic cells was subtracted to obtain the respective proportion of the cells, the committed by a particular treatment induced apoptosis. Each cell population was evaluated on

the basis of the created template coordinates and adds the values for the early apoptosis in connection.

2.2.5 Migration analysis with Wound-healing assay

2.2.5.1 Migration process

Cell migration is a complex process, both at the physiological wound healing, as well as in tumor formation in which metastasis plays an important role. A Wound-Healing assay mimics the directional cell migration, which takes place during wound healing. Thus it can be examined if the treatment with AF in comparison with the control has an inhibitory effect on the migration of the PDAC cells.

2.2.5.2 Experimental Procedure

Cell lines were seeded in a 6-well plate and left to reach 80% confluence. Initially, cells were starved for 24h in media containing 2% FCS. Then KP3 and Panc-1 cell lines were further incubated for 48hrs in the starvation media containing either the controls (DMSO) or AF. Afterwards a scratch was done using a 10µl white tip for each treatment. Then cells were washed with PBS and photographed using Leica DMI 6000 B microscope (Leica, Wetzlar, Germany). Cells were incubated for an additional 24h after which the photographs were taken for the wounded area. The migrating cells were calculated according to the following formula:

$$\text{Migration Index} = \frac{\text{Width of the wound}_{0h} - \text{Width of the wound}_{24h}}{\text{Width of the wound}_{0h}} \times 100$$

The width of the respective wound determined (there were 3 per measurement points per wound selected). For each treatment, the difference in wound diameter between time 0h and time 24hrs was determined and related to the

time 0h. Since each wound has several measuring points, an average was determined and the migration index.

2.2.6 Invasion measurement with BD Matrigel™ Invasion Chamber BioCoat™

2.2.6.1 BD Matrigel Invasion Chamber BioCoat

The membrane of the invasion chamber has 8µm large pores, which is covered by a thin Matrigel Basement membrane matrix. This is located between the FCS-free and the complete medium and serves as an artificial basement membrane which covers the pores, so that non-invasive cells are prevented from migrating through the pores. Invasive cells, attracted by the complete medium, however, can become detached from the membrane and invade through the pores.

2.2.6.2 Experimental Procedure

The invasion chamber (stored at -20°C) was warmed at RT and rehydrated after reaching RT with serum-free medium for 2 hrs in the incubator. Subsequently, the medium was aspirated and administered 2.5 ml complete medium in the environmental chamber. A total of 2.5×10^5 cells / 2ml were plated in the upper chamber filter in serum free media. The cells were treated simultaneously with AF (0.5µg/ml, 2µg/ml, 6µg/ml) and control (DMSO). The invasion assay utilized 6-well BD BioCoat™ Matrigel™ Invasion Chamber (BD Biosciences, Bedford, UK). These upper chamber filters were placed into the BD Falcon TC Companion Plate (BD Biosciences, Bedford, UK) containing 10% FCS. After 48 hrs incubation at 37°C, 5% CO₂ atmosphere the cells on the upper surface of the membrane were mechanically removed with cotton swab. The invading cells were fixed in 100% ice-cold methanol (AppliChem, Darmstadt) and stained with 1% toluidine blue (Sigma-Aldrich, St. Louis, USA)

in 1% borax (Sigma-Aldrich, St. Louis, USA). Cells were then counted under the microscope (Leica DM 5000 B, Wetzlar, Germany). The calculation of the invading cells was done according to the BD protocol. With a light microscope respectively cells were counted in 5 fields of view and made photos (40x magnification). The respective mean values were based on the average of the DMSO control and calculated as the invasion index.

$$\text{Invasion Index} = \frac{\% \text{ Invasion Test Cell}}{\% \text{ Invasion Control Cell}}$$

2.2.7 Soft Agar Assay

2.2.7.1 Soft agar colony formation

The soft agar colony formation assay is a technique widely used to evaluate cellular transformation *in vitro*. In this technique, cells were dispersed onto a culture plate and grown in the presence of 'feeder' cells or conditioned medium to provide necessary growth factors. In the traditional soft agar colony formation assay, cells are grown in a layer of soft agar mixed with cell culture medium that rests on another layer of soft agar, also mixed with cell culture medium, but containing a higher concentration of agar. This prevents cells from adhering to the culture plate, yet allows transformed cells to form visible colonies. The rationale behind this technique is that normal cells depend on cell to extracellular matrix contact to be able to grow and divide. Conversely, transformed cells have the ability to grow and divide irrespective of their surrounding environment. Therefore, cells able to form colonies in an anchorage-independent manner were considered to be transformed and carcinogenic.

2.2.7.2 Experiment Procedure

Before experiment, maintain the waterbath at 45°C. Make 50 ml of 5% Noble agar (Difco; BD Biosciences, Franklin Lakes, NJ) in water, autoclave to dissolve. When agar is melted, mix agar on stir plate, leave cool for 15 mins. To 120 ml of medium, add 30 ml of 5% agar, you will get 1% agar in the end. Soft agar plates were prepared in 6-well plates with bottom layer of 1% noble agar in complete culture medium. 6×10^4 cells/well were suspended in 3mL of 0.5% of agarose along with the different concentration of drug (AF) and control (DMSO) and were seeded as a top layer on to 1% agar coated plates. The cells were incubated for 2 weeks at 37°C in a humidified atmosphere containing 5% CO₂ and counterstained with p-iodonitotetrazonium violet (Sigma Aldrich, Germany). The number and size of colonies were determined after 3 weeks under the microscope.

2.2.8 Protein extraction and western blotting

Certain proteins in cell lysates can be detected using Western blotting. Proteins are separated by electrophoresis according to their molecular weight when transferred to a membrane. By means of specific antibodies the target protein can then be detected on the membrane. The peroxidase coupled to the secondary antibody converts the substrate luminol, chemiluminescent signals can be displayed on an X-ray film (according to manufacturer information).

2.2.8.1 Cell Culture

Panc-1 and KP3 cells treated with DMSO and AF (24hrs, 48hrs and 96hrs) were collected and transferred to 15ml test tubes and centrifuged for 5 min at 1000rpm. The supernatant was discarded, the cell pellet was resuspended with 1ml ice cold 1xPBS and centrifuged again. The supernatant was discarded and the cell pellets were incubated in 200µl Western lysis buffer buffer supplemented by protease and phosphatase inhibitors for 30mins on

ice. In addition, sonification was made the on ice then the sonification was made the on ice (twice each 15 seconds per cell pellet) for the destruction of the intact cell walls. Thereafter, the suspensions were centrifuged for 25 min at 13000Rpm and 4°C. The supernatant containing the cell lysate was carefully transferred into Eppendorf tubes and determined the protein content.

2.2.8.2 Determination of protein concentration

The protein determination was carried out according to manufacturer's instructions with the DC Protein Assay (BioRad). The proteins react with the alkaline copper tartrate solution and Folin reagent, this leads to a color change. The absorbance (650nm) was measured with the Micro plate-Reader Multiskan Plus (Titertek-Berthold, Pforzheim, Germany). The mean value of the protein sample from the triplicate well was used for analysis. The amount of cell lysate in 1µl calculated as follows: $100 / ((x-0.0627) / 0,136)$. It was filled with western lysis buffer to 100 µl by adding 25µl 4x protein loading buffer.

2.2.8.3 Preparation of separating and stacking SDS polyacrylamide gels

The separating gel was poured between two glasses plates sealed with 100% ethanol. After 30 mins, the ethanol was removed. The stacking gel was poured on top of the separating gel.

2.2.8.4 Electrophoresis

The gel was placed into the electrophoresis chamber and filled with 1×SDS running buffer. Before the samples were loaded, they were boiled for 5 min at 95 °C and then centrifuged. As protein markers page ruler plus prestained protein ladder (Fermentas) was used. Electrophoretic separation was conducted at 80V until the separating gel was reached, then the voltage was increased to 120V.

2.2.8.5 Protein transfer to PVDF membrane

The PVDF membrane was briefly incubated in 100% methanol, and then put in 1x western transfer buffer. When assembling the Blotting-sandwiches (holder / sponge / Watman filter paper / gel / PVDF membrane / Watman filter paper / sponge / holder) bubbles were pushed away thoroughly. The protein transfer was performed at 4 ° C, 0,35mA and 100V for one hour. Subsequently, the PVDF membrane was shifted to blocking solution (5% dried milk AppliChem, Darmstadt, Germany) for one hour and then washed with 1xTNT Buffer on the shaker.

2.2.8.6 Antibody incubation and development

After washing, the membranes were probed with primary antibodies against E-cadherin (1:1000; Cell signaling, 24E10), N-cadherin (1:50,000; Millipore, EPR1792Y), Actin (2:10.000; Sigma, AC-74), p27^{kip1} (1:500; Santa Cruz Biotechnology, C-19), p21^{waf1/cip1} (1:500; Santa Cruz Biotechnology, sc-6246) overnight. The next day membrane was washed three times for 10 min with 1xTNT washbuffer and then incubated for 1 hour at RT with the secondary antibody. After another three washes with 1xTNT wash buffer the PVDF membrane were exposed to Amersham Hyperfilm ECL (GE Healthcare Limited Buckinghamshire, UK), ECL-films were placed on the membrane and this developed after an exposure time of 1-5 min in the dark.

2.2.9 Cell Senescence assay

2.2.9.1 X-gal

Senescence-associated β -galactosidase activity is a widely used biomarker for assessing replicative senescence in mammalian cells. This enzymatic activity has generally been measured by staining cells with the chromogenic substrate

5-bromo-4-chloro-3-indolyl- β -d-galactopyranoside (X-gal) at pH 6.0, a reaction condition that suppresses lysosomal β -galactosidase activity sufficiently to ensure that most non-senescent cells will appear unstained.

2.2.9.2 Experiment Procedure

To determine the senescence, cells were seeded (2×10^4 /ml) in six well plate and were further treated under the same conditions described for WST-1 assay. After the respective treatment cells were fixed with 0.5% glutaraldehyde solution (in PBS, pH 7.4) for 5min at RT. Followed by washing with PBS once and twice with PBS/MgCl₂ (pH 5.5) for 5 min at RT. Freshly prepared X-gal solution containing PBS/MgCl₂, 0.2M K₃Fe[8]₆, 0.2M K₄Fe[8]₆, X-Gal stock (40x) (Peqlab; 37-2610) was added to the cells. The cells were incubated at 37° C for few hrs sealed and protected from light. After staining the cells for desired intensity, the cells were washed three times with PBS for 5 min. Post fixed with 4% Formalin in PBS for 30 min at RT followed by washing for three times with PBS at RT. Pictures were taken and the stained cells were counted under the microscope (Leica DM 5000B, Leica Wetzlar). The percentage of positive cells (of the total cell number) in the treated sample was determined and plotted.

2.2.10 Cell Cycle

2.2.10.1 Cell-cycle analysis using propidium iodide staining and flow cytometry

Cell cycle analysis is a method in cell biology that employs flow cytometry to distinguish cells in different phases of the cell cycle. Before analysis, the cells are permeabilised and treated with a fluorescent dye that stains DNA quantitatively, usually PI. The fluorescence intensity of the stained cells at certain wavelengths will therefore correlate with the amount of DNA they contain. As the DNA content of cells duplicates during the S phase of the

cell cycle, the relative amount of cells in the G₀ phase and G₁ phase (before S phase), in the S phase, and in the G₂ phase and M phase (after S phase) can be determined, as the fluorescence of cells in the G₂/M phase will be twice as high as that of cells in the G₀/G₁ phase. Cells with fractional DNA contents, a situation occurring during apoptosis, can be identified as a “sub-G₁” population, the presence of a sub-G₁ peak in the fluorescent signal is often interpreted as a loss of DNA due to its fragmentation associated with apoptosis. Cell-cycle anomalies can be symptoms for various kinds of cell damage, for example DNA damage, which cause the cell to interrupt the cell cycle at certain checkpoints to prevent transformation into a cancer cell (carcinogenesis). Other possible reasons for anomalies include lack of nutrients, for example after serum deprivation.

2.2.10.2 Experiment Procedure

2x10⁵ Panc-1 and KP3 cells were treated cultured with AF treatment (48hrs and 96hrs). First wash with 1xPBS and trypsinized them resuspended in medium + 10% FCS, centrifuged (1000 rpm, 5 mins). Pellet were resuspended in 1ml 1xPBS and centrifuge again. Then Pipet cells were fixed in suspension into 3 ml absolute 80% Ethonal overnight at -20°C, keep vortexing in order to prevent clustering of cells during the fixation. Incubate on ice for 15 min (or over night at -20°C).The next day pellet the cells at 1500 rpm for 5 mins. Suspend the pellet in 500 µl PI-solutionin-PBS: 50 µg/ml PI from 50x stock solution (2.5 mg/ml) 0.1mg/ml RNase A and Incubate for 40 min at room temperature following flow cytometry analysis.

2.2.11 Animals and treatment

2.2.11.1 Animals and genotyping analysis

Therapeutic studies *in vivo* were performed with Pdx1- Cre; LSL-Kras^{G12D}; p53^{lox/+} mice (KPC Mouse model) which have been previously described [53]. The transgenic Pdx1-Cre mice and p53^{lox/+} mice were obtained from Aram Hezel (University of Rochester Medical Center, USA). Kras mice were kindly provided by Lars Zender (UKT, Germany). The mice were crossed and genotyped to obtain the mice with background Pdx1-Cre; LSL-Kras^{G12D}; p53^{lox/+} (according to 2.1.6.3).

2.2.11.2 Drug and treatment *in vivo*

A total of 18 mice were used for the *in vivo* experiment. We initiated an animal trial with 6 mice per treatment group. Mice were treated intraperitoneally with AF (1mg/kg/body weight, Day1-Day3), a combination of AF (1mg/kg/body weight Day1-Day3) + Gemcitabine (100mg/kg/body weight Day 5) or vehicle(PBS) starting at an age of 14-weeks (Figure.5). The mice were sacrificed when critical illness was developed; sizes of pancreas and visible tumor were measured by caliper and organ tissues were harvested. Tumor volume was calculated using the following formula: Tumor volume $V = \frac{(\pi/6) \times (\text{Length}) \times (\text{Width}^2)}$. The tumor tissues were snap frozen for protein analysis and fixed in 4% formalin for histology. The other organs were collected for further histological analysis. All animals were analyzed for metastases and ascites.

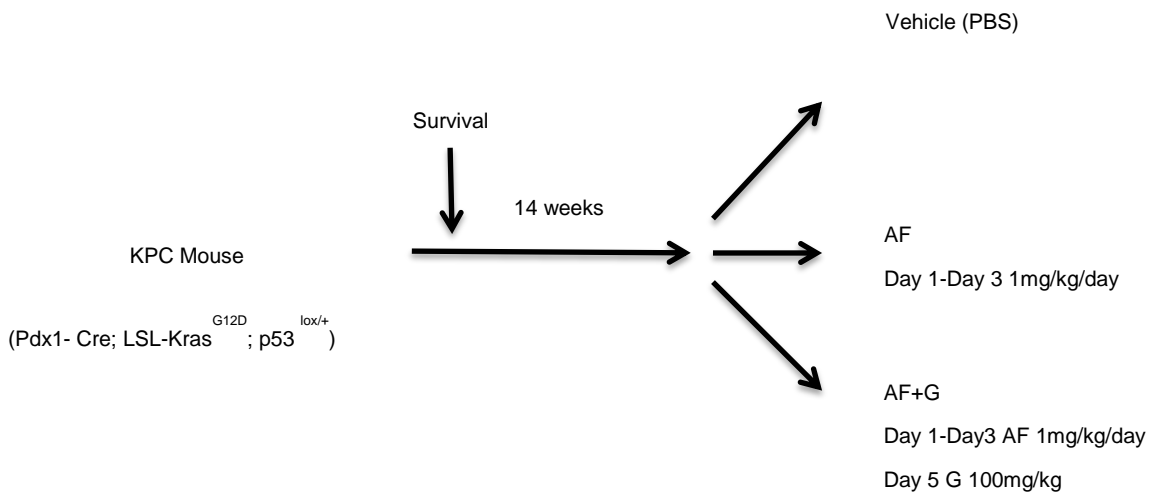


Figure.5 Design for survival experiment

2.2.12 Immunohistochemistry

2.2.12.1 The principle of immunohistochemistry

Immunohistochemical staining allows antigens in tissue sections being demonstrated. In the indirect method, a specific primary antibody binds to the antigen and in doing so it can bind a secondary antibody. The visualization of these bindings is done by the Avidin-Biotin-Complex (ABC) method: Avidin binds biotin with the coupled secondary antibody. The colorless 3,3'-diaminobenzidine (DAB) is activated by binding to the biotin-avidin-peroxidase complex and assumes a brown color, so ultimate the antigen is visible.

2.2.12.2 Experimental Procedure

Tissue sections were fixed in 4% formalin (Sigma-Aldrich, St. Louis, USA) overnight, stored in PBS and embedded in paraffin. But they were incubated overnight in the hybridization oven at 55 ° C before experiment. The remaining paraffin was removed by the incubation in xylene. Thereafter, the sections were rehydrated with graded concentrated alcohol (6 min to 100%, 95%, 75%, 40% ethanol) and then rinsed three times for 3-5 min with 1xPBS. Because

some proteins are cross-linked by the formalin fixation, they can not be detected. In order to establish their spatial structure again, the vapor pressure method was used. But the slides were put in a pressure cooker filling with antigen Unmasking Solution (Vector Laboratories) / autoclaved water (1: 100 dilution) dipped. After the water has been brought to a boil, was 15 to 20 min waiting, only to reduce the pressure by running cold water and gently remove the sections. Then they were rinsed three times for 3-5 min and then put into 1% hydrogen peroxide / water for 10 min. The sections were washed again three times for 3 min each in 1×PBS, and then overlap 100 µl blocking solution (5% normal serum + 0.3% Triton X-100, Vector Laboratories, Inc., Burlingame), cover with parafilm and incubate for one hour in a horizontal dark box at RT. The tissue was then incubated with 100 µl of primary antibody / blocking solution (1:100 dilution) overnight at 4°C. The primary antibody Ki-67 (1:100; Novacastra,U.K.), CD34 (1:100; Novusbio,NBP1-44407,EP373Y) was carried out in this experiment. The next day the sections were washed three times for 3 min each in 1×PBS and then incubated in 100 µl each secondary antibody Rabbit (1:200,Vector Laboratories, Inc., Burlingame) / blocking solution for 1 hour at RT. The sections were then rinsed three times for 3 min with 1 × PBS, 100 µl of ABC reagent (Vectastain ABC Kit, Vector Laboratories) was applied to the tissue and incubated for one hour after the above-mentioned principle. Three times in 1 × PBS rinse each 300 ul freshly prepared Vector DAB substrates (peroxidase Substrate Kit DAB, Vector Laboratories) were applied to the fabric and waited up to 3 min until a brownish color was visible. Subsequently, the slides were immersed in distilled water to stop the DAB reaction. This was followed by counterstaining with hematoxylin for 1 minute and subsequent rinsing with water. Finally, the slides were rinsed in ascending alcohol series for dehydration (three min each in 40%, 75%, 95% and 100% ethanol) and for 6 min were immersed in xylene. For the

quantification of Ki-67 staining, we use imagejsl.org online software to make the analysis. For the CD34 microvascular quantification we use MVD (microvascular density) assay, the MVD areas were quantitatively measured by Image-Pro plus 6.2.1 software (Media Cybernetics, Silver Spring, EUA). The final MVD of each sample was calculated by the ratio of the sum of the immunopositive areas and the sum of the total area.

2.2.13 Statistical Analyses

All the experiments were repeated 3 times. Data are presented as mean±standard deviations [39]. The results were analyzed using software Graphpad prism version 5.0 (GraphPad Software, San Diego, CA, USA) and SPSS Version 11.0 (SPSS, Chicago, USA). The tests include one-way ANNOVA analysis of variance and student's *t*-test along with Bonferroni post test and paired and unpaired *t*-tests. The overall survival analysis using Kaplan-Meier curves were analysed by log rank test. For all tests, a P value of <0.05 was considered statistically significant.

3. Results

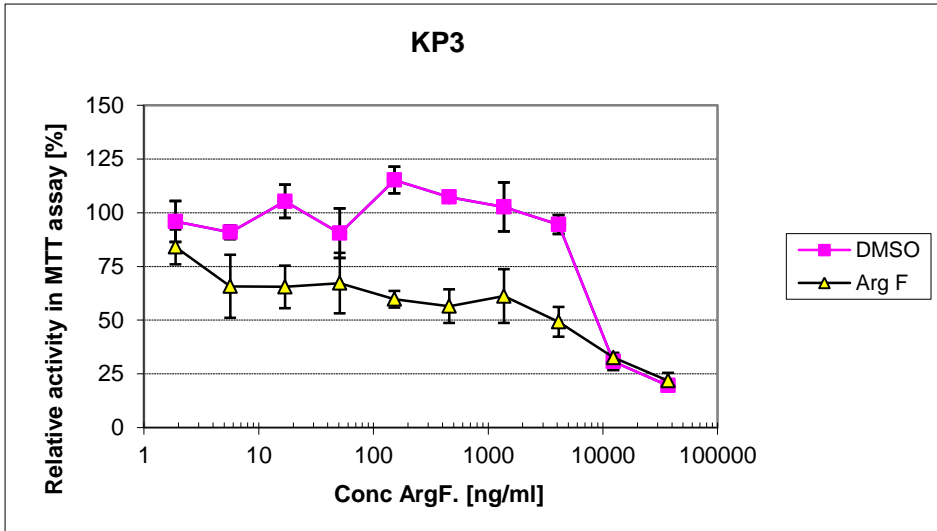
3.1 Argyrin F (AF) treatment inhibits proliferation, migration, invasion and colony formation of human PDAC cell lines

First, we determined the sensitivity of the KP3 and Panc-1 cell lines to AF treatment by WST-1 assay. Cells were submitted for 72hrs to a range of AF concentrations going from 0.001 μ g/ml to 100 μ g/ml. Panc-1 showed higher sensitivity to AF with a half maximal inhibitory concentration (IC_{50}) equal to 0.5 μ g/ml and KP3 exhibited lower ($IC_{50} = 6\mu$ g/ml) (Figure.6). Thus, we continued with three different concentrations of AF for *in vitro* experiments: 0.5 μ g/ml, 2 μ g/ml and 6 μ g/ml. Next, cell proliferation assays showed AF treatment reduced the number of viable KP3 and Panc-1 cells in a dose and time dependent manner (Figure.7, Figure.8). The light-microscopic pictures were taken after 96hrs, respectively illustrate the inhibitory effect of AF on the growth of PDAC cell lines.

The metastasis process of malignant neoplasms is due the ability of migration and invasion of malignant cells. Thus, we sought to explore the impact of AF on this process in KP3 and Panc-1 cells lines. First, we examined cell motility by employing wound healing assays in the presence or absence of AF. 24hrs after the scratch, cell migration into the wound was captured under the microscope at 10x magnification (Figure.9, Figure.10). For both KP3 and Panc-1 cells, significant inhibition of wound closure was seen with treatment of 6 μ g/ml AF ($p < 0.05$). In contrast, 80-90% wound healing was seen after 24hrs in all DMSO control cells. Thus, AF can effectively inhibit the migration of PDAC cells. Next, we tested cell invasion by using transwell chambers. PDAC cells were plated in wells of an invasion chamber in the presence of different drug concentrations compared to DMSO control and experiments were conducted in Material and Methods. As shown in Figure.11 and

Figure.12, the invasion of PDAC cells (KP3, Panc-1) was significantly reduced ($p < 0.05$) upon treatment with AF, with reductions of up to 60% - 70% in the number of invading cells compared to the DMSO control group. In particular for KP3 cells, the concentration of 0.5 μ g/ml showed no significant difference compared to the DMSO control. Thus, treatment with AF has an anti-invasive effect on human PDAC cell lines. Finally, AF strongly inhibited the ability of both pancreatic cells to form colonies in soft agar compared to DMSO treated cells. (Figure.13, Figure.14). These experiments suggest that AF treatment can inhibit proliferation, migration, invasion and colony formation of human PDAC cell lines. Panc-1 cells showed overall stronger inhibitory effect under AF treatment compared to KP3 cells.

a.



b.

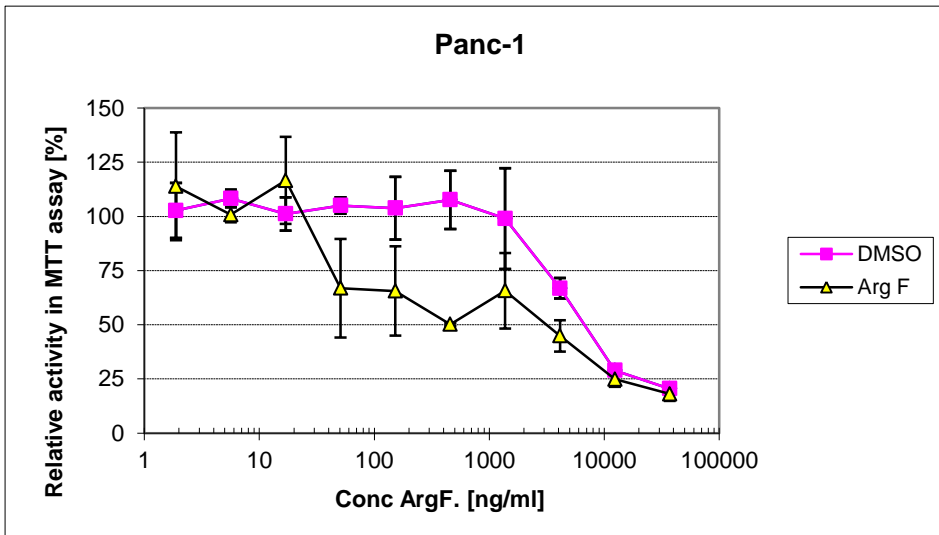
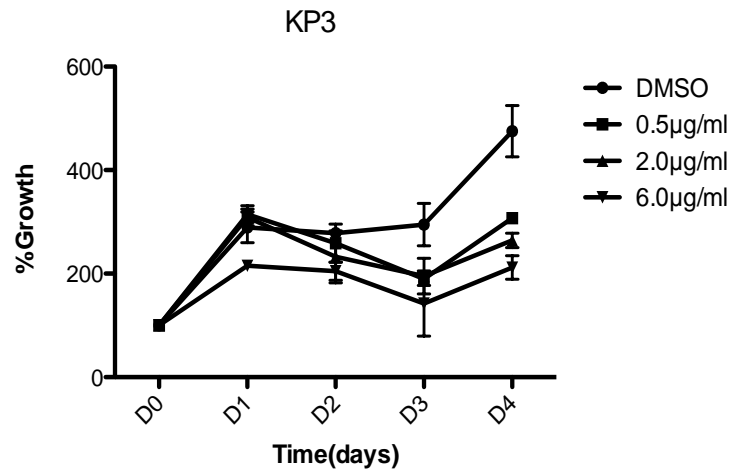


Figure.6 **Argyrin F cytotoxicity**

(a) KP3 and (b) Panc-1 cells were treated for 72hrs with increasing concentrations of AF (0,001 μ g/ml to 100 μ g/ml). Cell viability was measured using WST-1 assay and DMSO was used as the control.

a.



b.

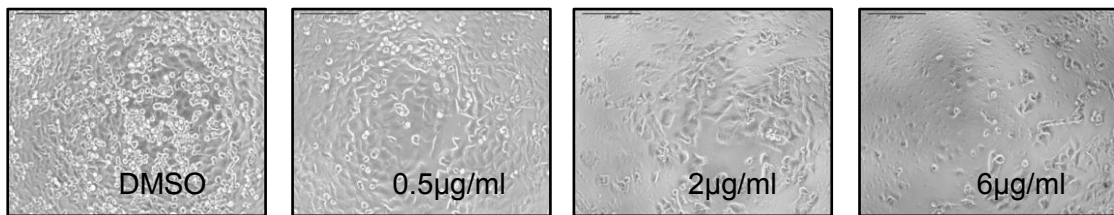


Figure.7 **WST-1 assay: Dose-dependent inhibition of cell proliferation of KP3 by AF**

a. Representation of the proliferative growth of the respective treatments. Shown with mean values and standard deviations; b. Comparative presentation of the corresponding light microscopic images: 10x magnification

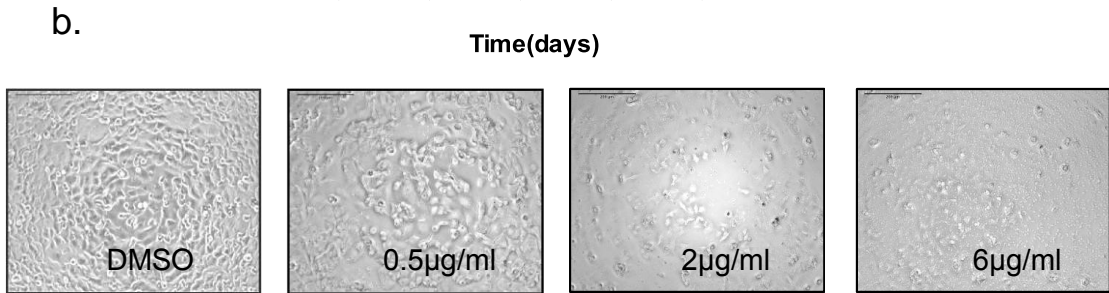
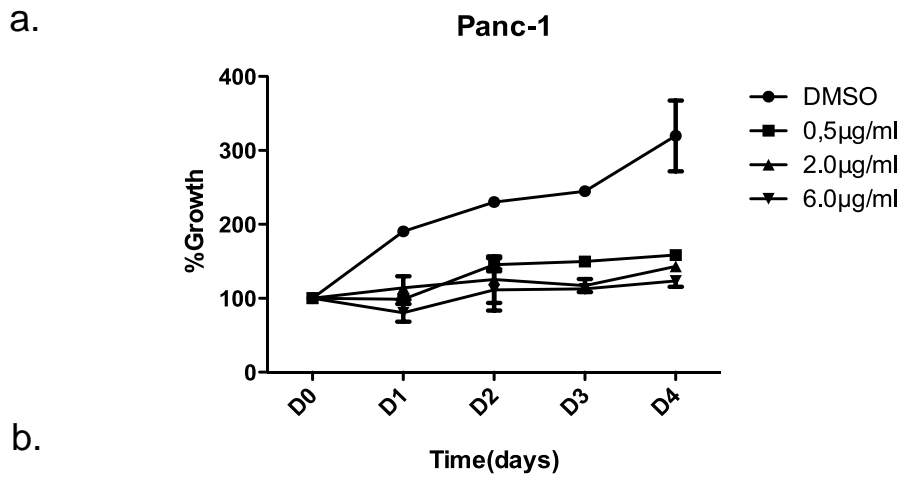
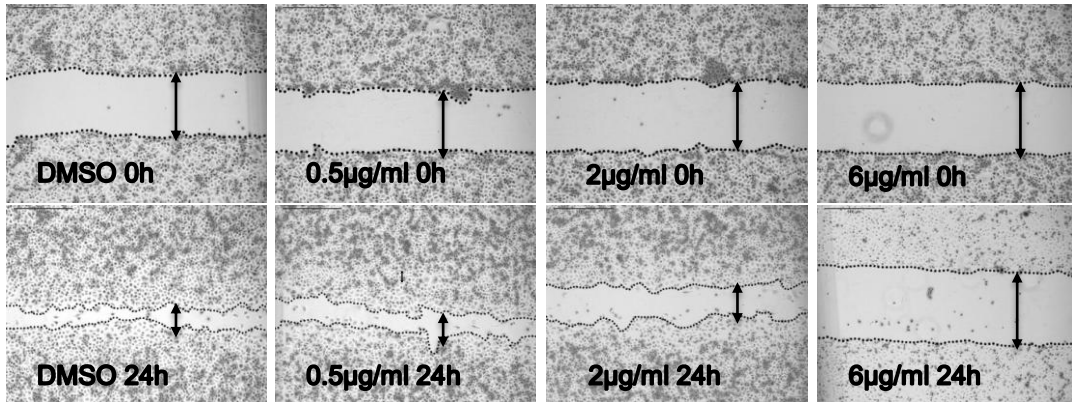


Figure.8 **WST-1 assay: dose-dependent inhibition of cell proliferation of Panc-1 by AF**

a. Representation of the proliferative growth of the respective treatments. Shown with mean values and standard deviations; b. Comparative presentation of the corresponding light microscopic images: 10x magnification

a.



b.

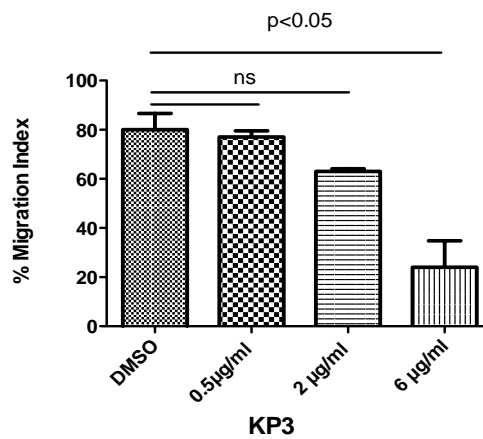
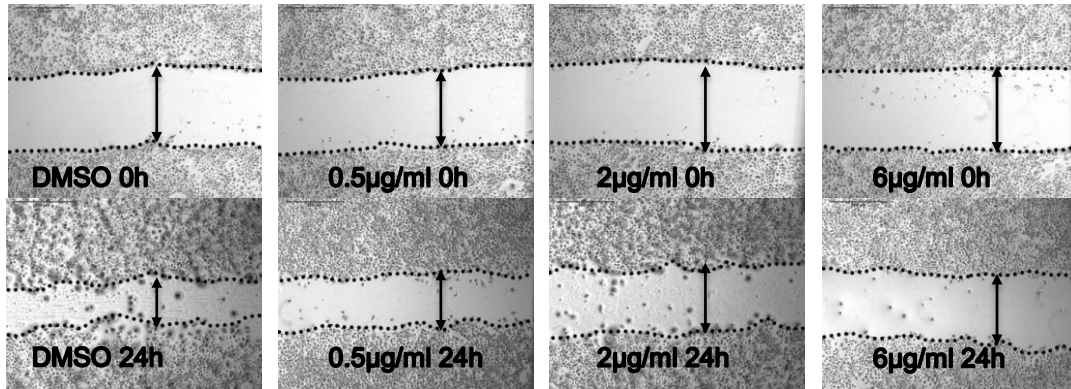


Figure.9 Inhibition of cell migration on KP3 cell by AF treatment

a. Wound healing experiments were done for KP3 cells cultured with DMSO and AF (0.5 µg/ml, 2 µg/ml and 6 µg/ml). The dotted lines and arrows are representing the edges of the wound. Photographs were taken at 0 and 24hrs under light microscope (10x magnification). b. The migration index was calculated as described in Materials and methods and plotted in bar graphs. Differences were considered as statistically when the p-value<0.05 and ns when p-value>0.05. The error bar represents standard deviation.

a.



b.

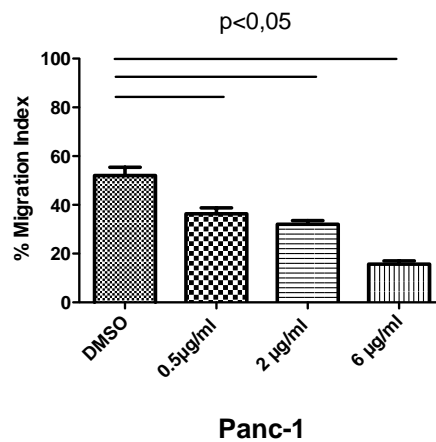
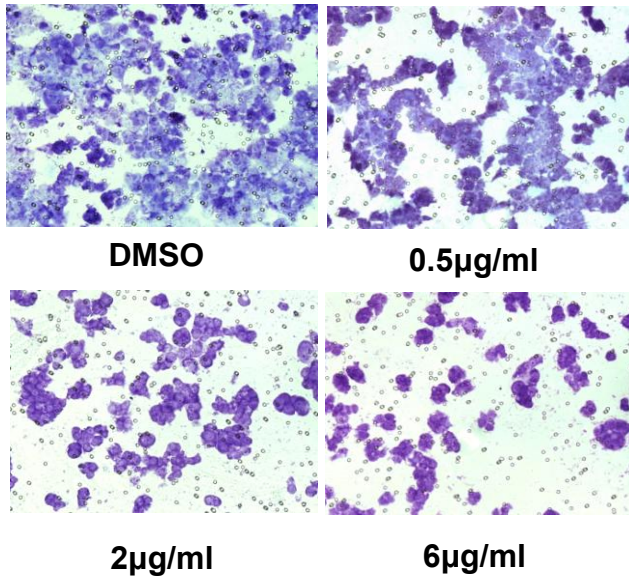


Figure.10 Inhibition of cell migration on Panc-1 cell by AF treatment

a. Wound healing experiments were done for Panc-1 cells cultured with DMSO and AF (0.5 µg/ml, 2 µg/ml and 6 µg/ml). The dotted lines and arrows are representing the edges of the wound. Photographs were taken at 0 and 24hrs under light microscope (10x magnification). b. The migration index was calculated as described in Materials and methods and plotted in bar graphs. Differences were considered as statistically when the p-value < 0.05 and ns when p-value > 0.05. The error bar represents standard deviation.

a.



b.

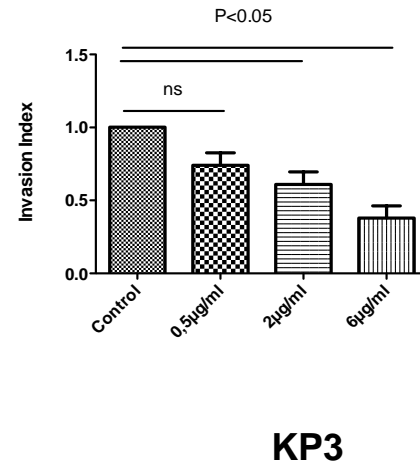


Figure.11 Inhibition of invasion on KP3 cell by AF treatment

a. KP3 cells were treated as indicated previously for 48hrs to investigate the effect on invasiveness. The number of cells that invaded through the membrane was determined by light microscope (20x magnification). b. Invasion index was calculated as described in Materials and methods and plotted in bar graphs. Differences were considered as statistically significant when the p-value<0.05 and ns when p-value>0.05. The error bar represents standard deviation.

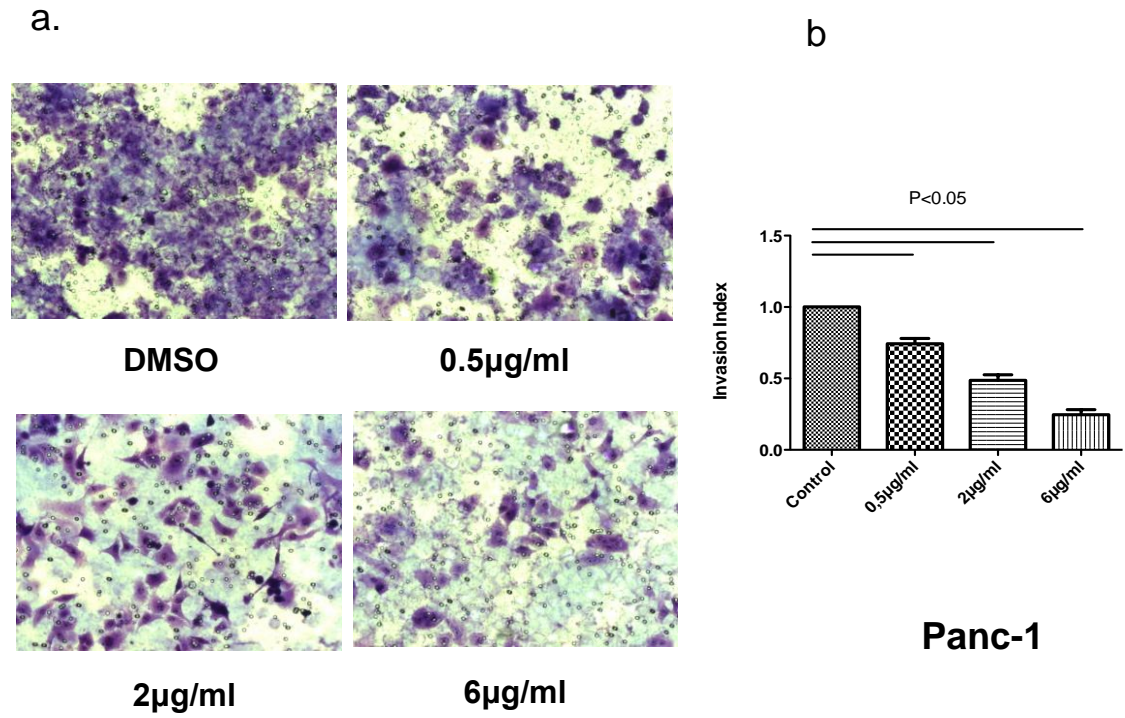
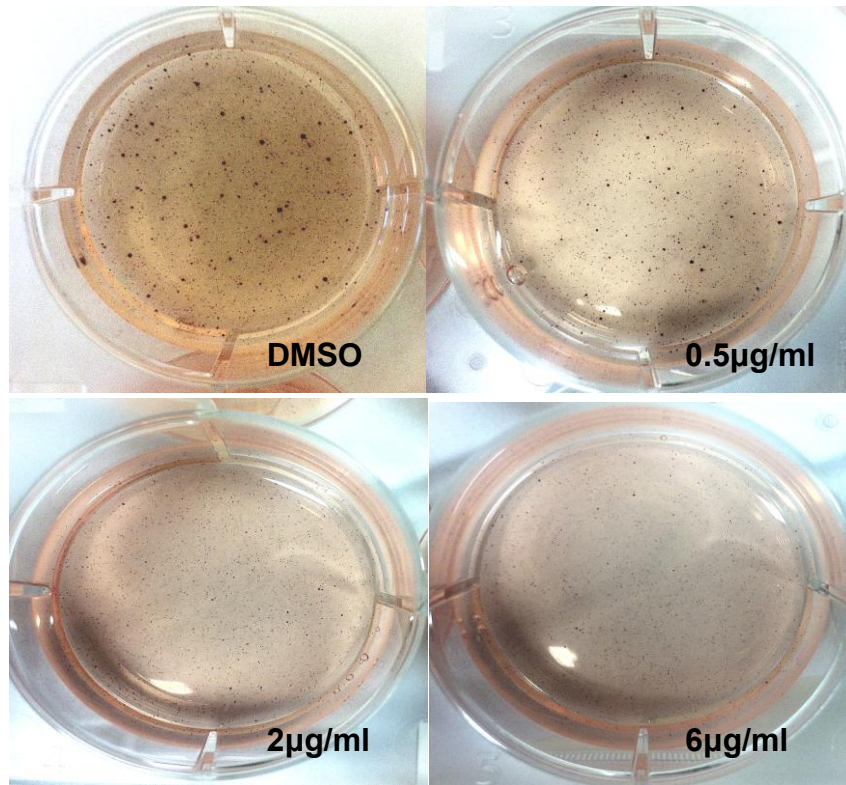


Figure.12 Inhibition of invasion on Panc-1 cell by AF treatment

a. Panc-1 cells were treated as indicated previously for 48hrs to investigate the effect on invasiveness. The number of cells that invaded through the membrane was determined by light microscope (20x magnification). b. Invasion index was calculated as described in Materials and methods and plotted in bar graphs. Differences were considered as statistically significant when the p-value<0.05 and ns when p-value>0.05. The error bar represents standard deviation.

a.



b.

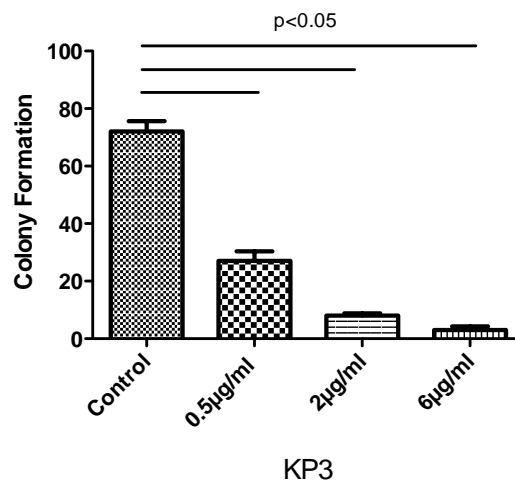
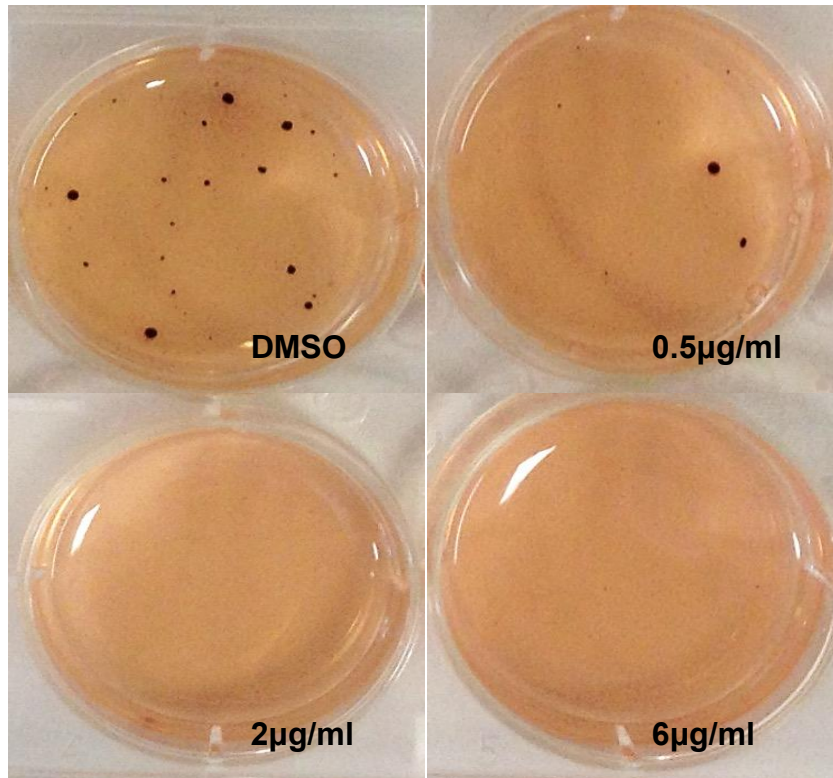


Figure.13 Inhibition of colony formation on KP3 cells by AF treatment

a. KP3 cells were treated as indicated for 3 weeks under DMSO and AF (0.5 µg/ml, 2 µg/ml and 6 µg/ml). The numbers of colonies were determined by light microscope (10x magnification). b. The number of colonies were calculated when its diameter was >0.75cm and plotted in bar graphs. Differences were considered as statistically when the p-value < 0.05 and ns when p-value > 0.05. The error bar represents standard deviation.

a.



b.

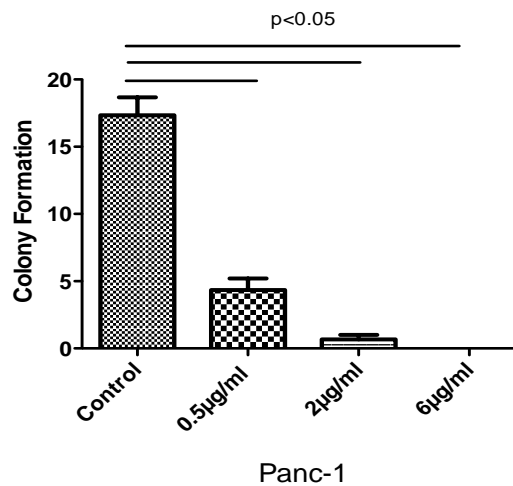


Figure.14 Inhibition of colony formation on Panc-1 cells by AF treatment

a. Panc-1 cells were treated as indicated for 3 weeks under DMSO and AF (0.5 µg/ml, 2 µg/ml and 6 µg/ml). The numbers of colonies were determined by light microscope (10x magnification). b. The numbers of colonies were calculated when its diameter was >0.75cm and plotted in bar graphs. Differences were considered as statistically when the p-value < 0.05 and ns when p-value > 0.05. The error bar represents standard deviation.

3.2 Argyrin F(AF) treatment induces considerable apoptosis compared to senescence in human PDAC cell lines

In order to analyze whether AF treatment induces apoptosis in PDAC cells we first performed Annexin V and PI staining. We found that AF treatment induced considerable levels of apoptosis in these PDAC cell lines, with levels increasing drug dose, but only 6µg/ml of AF showed significant induction of apoptosis compared to DMSO control ($p < 0.05$) (Figure.15). Higher induction of apoptosis up AF treatment was found in KP3 cells at 96hrs compared to Panc-1 cells (35% in KP3 and 16% in Panc-1).

Senescence is regarded as a physiological response of cells to stress, including telomere dysfunction, aberrant oncogenic activation, DNA damage, and oxidative stress [54]. Thus, we analyzed senescence as a possible cell death mechanism induced by AF. Relative percentage of senescence cells was measured by senescence associated β -galactosidase (SA- β -Gal) activity assay in KP3 and Panc-1 cells. PDAC cells were treated with DMSO and AF for 48hrs. As shown in Figure.16 and Figure.17, Panc-1 cells induced maximum of 10% of senescent cells at 6µg/ml of AF treatment compared to DMSO control, KP3 cells showed maximum of 9% induction of senescent cells in relation to DMSO control at 2µg/ml of AF treatment. No senescence was observed at 96hrs upon AF treatment (data not shown). Therefore, our results indicate that AF treatment mainly induces apoptosis in PDAC cells.

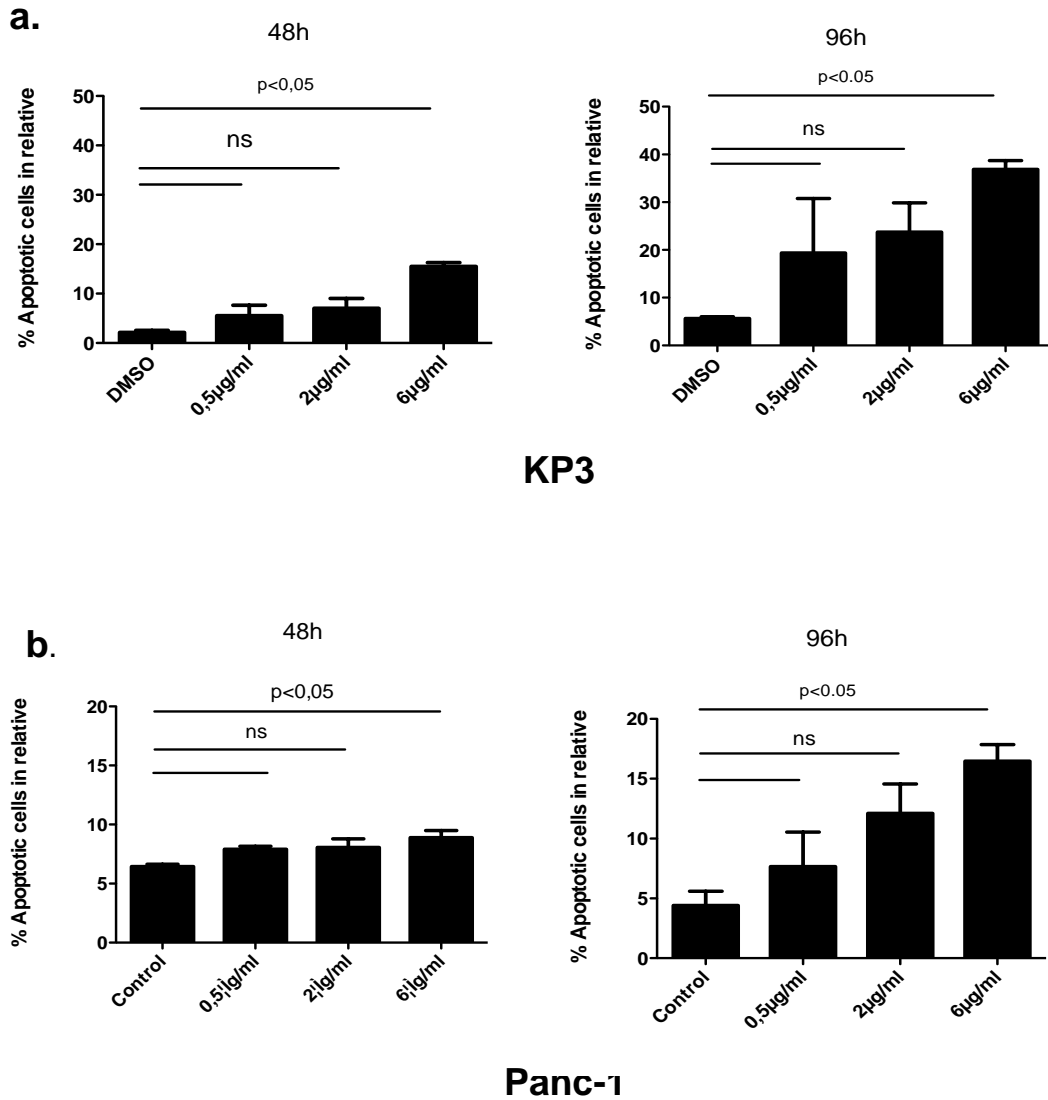


Figure.15 **AF treatment resulted in a considerable apoptosis for PDAC cells lines**

(a) KP3 cells and (B) Panc-1 cells treated with DMSO, or AF (0.5µg/ml, 2µg/ml, 6µg/ml) for 48hrs and 96hrs, the apoptosis was quantified by staining with Annexin V and propidium iodide (PI) using flow cytometry. Differences were considered as statistically when the p-value<0.05 and ns when p-value>0.05. The error bar represents standard deviation.

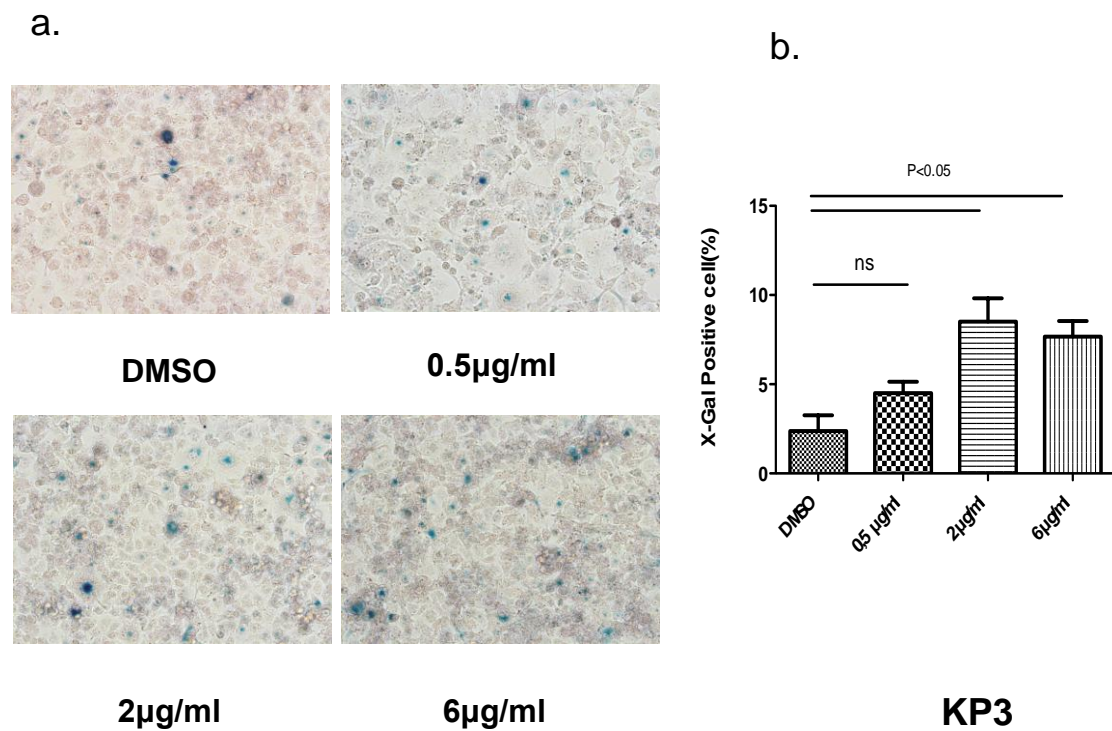


Figure.16 **AF treatment resulted in a partial induction of cellular senescence for KP3 cell**

a. KP3 cells were treated with DMSO, AF (0.5 $\mu\text{g/ml}$, 2 $\mu\text{g/ml}$, 6 $\mu\text{g/ml}$) for 48h and senescence was quantified by SA-beta-gal staining. B. The senescence positive cells were counted and plotted in bar graph. Differences were considered as statistically significant when the p-value was < 0.05 and ns was when p-value>0.05. The error bar represents standard deviation.

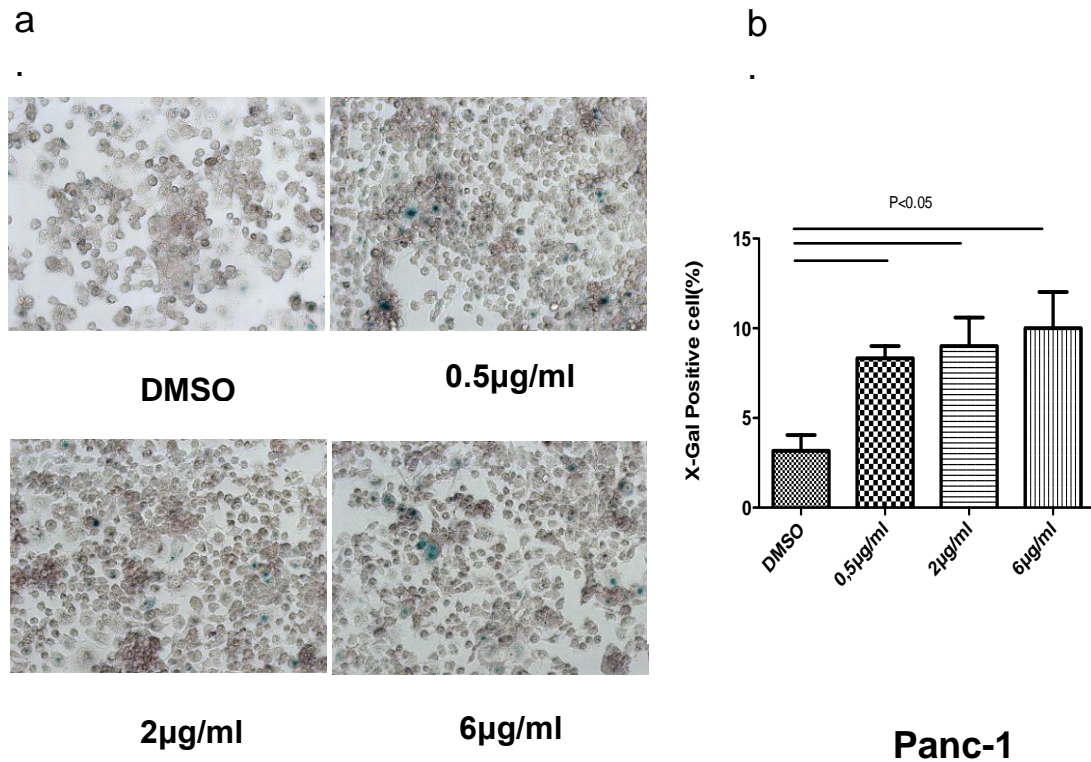


Figure.17 AF treatment resulted in a partial induction of cellular senescence for Panc-1 cells

a. Panc-1 cells were treated with DMSO, AF (0.5 μg/ml, 2 μg/ml, 6 μg/ml) for 48h and senescence was quantified by SA-beta-gal staining. B. The senescence positive cells were counted and plotted in bar graph. Differences were considered as statistically significant when the p-value was < 0.05 and ns was when p-value > 0.05. The error bar represents standard deviation.

3.3 Argyrin F (AF) treatment partially impairs epithelial-mesenchymal transition (EMT) in human PDAC cell lines

The epithelial-to-mesenchymal transition (EMT) is a process during which cells undergo a developmental switch from an epithelial phenotype to a mesenchymal phenotype [42]. In order to further examine whether AF can

attenuate EMT in human PDAC cell lines we treated KP3 and Panc-1 cells with different AF concentrations (0.5µg/ml, 2µg/ml, 6µg/ml) for 48 and 96hrs. For KP3 cells, we observed that epithelial marker (E-cadherin) was down regulated after 24hrs and the effect was stable till 96 hrs. But the expression of mesenchymal marker (N-cadherin) remained unchanged. For Panc-1 cells, pharmacological treatment resulted in an increased expression of E-cadherin and decreased expression of N-cadherin in a time-dose-independent manner as assessed by Western Blot (Figure.18). The results suggested that AF treatment might not have direct impact on EMT in PDAC cells.

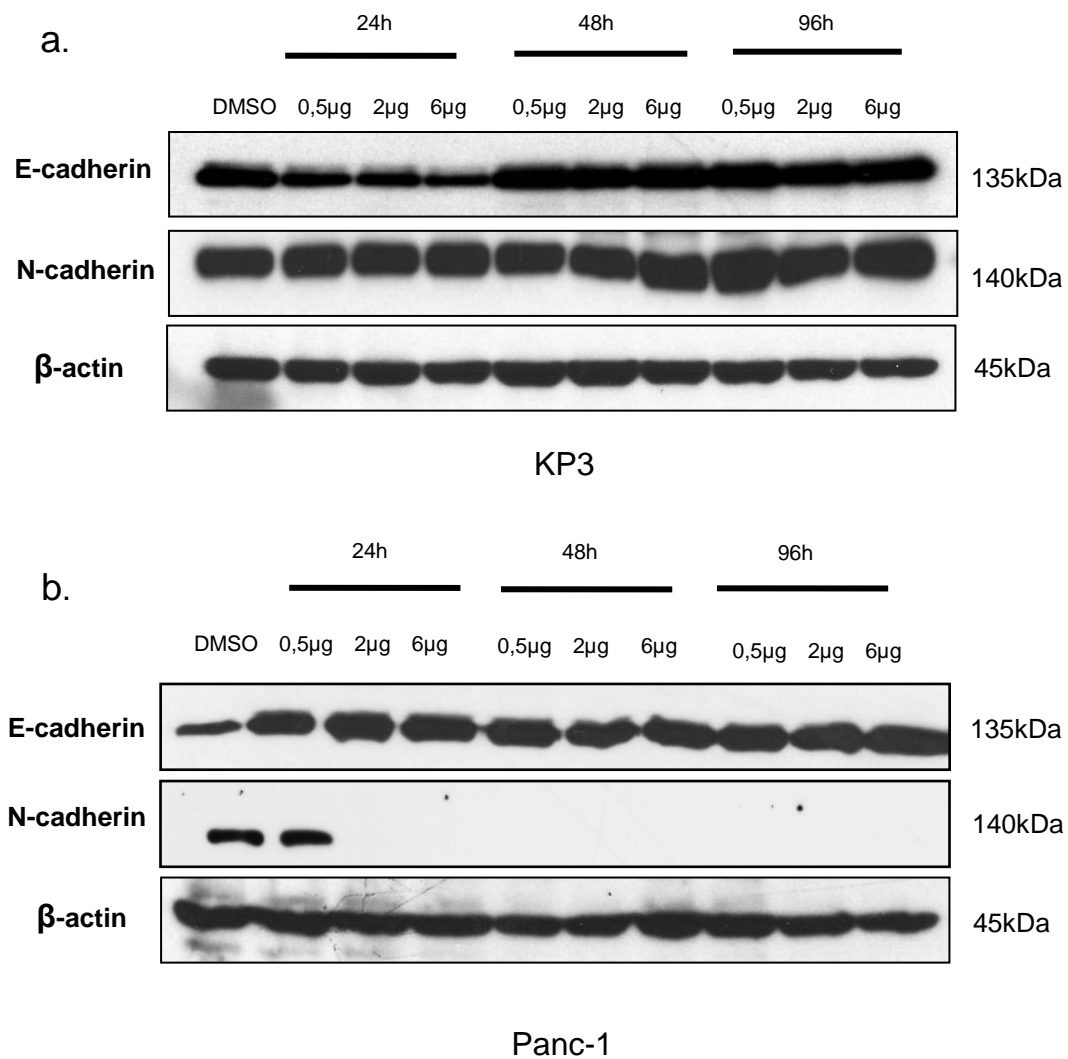


Figure.18 **AF treatment partially impairs EMT in PDAC cell lines**

(a) KP3 and (b) Panc-1 cells were treated with DMSO and AF (0.5μg/ml, 2μg/ml, 6μg/ml) for 48 and 96hrs. The expressions of EMT markers (E-cadherin and N-cadherin) were analyzed by western blot. β-actin was used as a loading control.

3.4 The effect of AF treatment on p27^{kip1} and p21^{waf1/cip1} and on cell cycle distribution in human PDAC cell lines

p27^{kip1} and p21^{waf1/cip1} are known to be important markers for cell cycle distribution [49]. Thus, we first checked the expression of of both of these markers p27^{kip1} and p21^{waf1/cip1} on protein level as assessed by Western Blot.

We found an effective upregulation of p27^{kip1} and p21^{waf1/cip1} under AF treatment compared to the respective DMSO controls in a time-dose-dependent manner in both PDAC cell lines (KP3, Panc-1) (Figure.19).

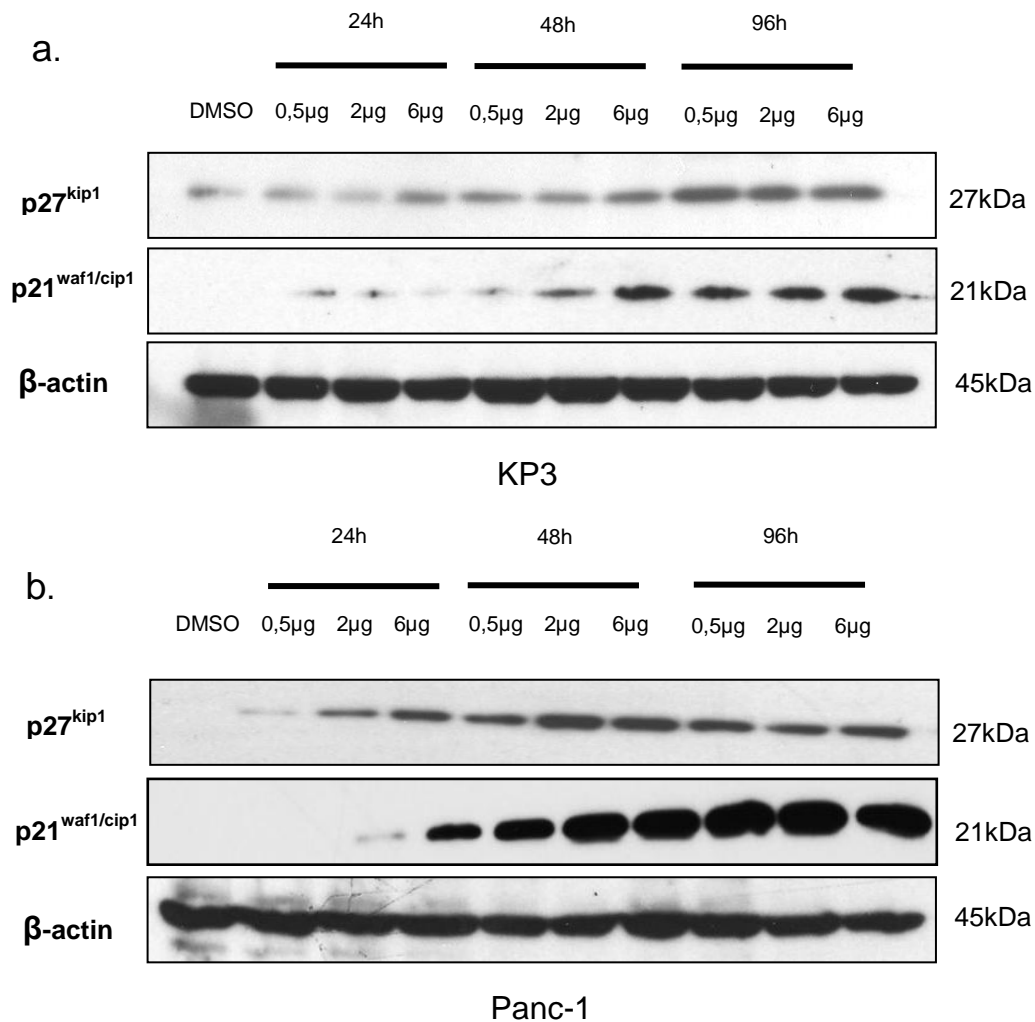


Figure.19 AF treatment showed stabilization effect on the expression of p27^{kip1} and p21^{waf1/cip1} levels in PDAC cell lines

(a) KP3 and (b) Panc-1 cells were treated with DMSO and AF (0.5µg/ml, 2µg/ml, 6µg/ml) for 48hrs and 96hrs. The expression of p27^{kip1} and p21^{waf1/cip1} were analyzed by western blot. β-actin was used as a loading control.

Subsequently, the effect of AF on the cell cycle distribution was examined. As shown in Figure.20, when exposed to AF treatment (0.5 μ g/ml, 2 μ g/ml, 6 μ g/ml), Panc-1 cells showed no increase in sub-G₁ population at 48hrs (1.8%, 1.19%, 1.64%) and 96hrs (1.93%, 1.75%, 2.14%) compared to DMSO (2.04%, 1.98%). But for KP3 cells, we found a considerable increase in percentage of sub-G₁ population as compared to DMSO (DMSO: 3.51%, 0.5 μ g/ml: 6.81%, 2 μ g/ml 8.30%, 6 μ g/ml: 9.12%) at 96hrs (Shown in Figure.20-a). The effect of AF treatment on KP3 and Panc-1 cell cycle distribution is shown in Table.1. There were progressively more cells in G₁-phase and fewer cells in S-phase at 48hrs and 96hrs for Panc-1, indicating a complete G₁/S phase arrest by AF treatment in a dose dependent manner. In contrast, KP3 cells showed no significant G₁/S-phase arrest when exposed to AF treatment at 48hrs and 96hrs (Figure.21).

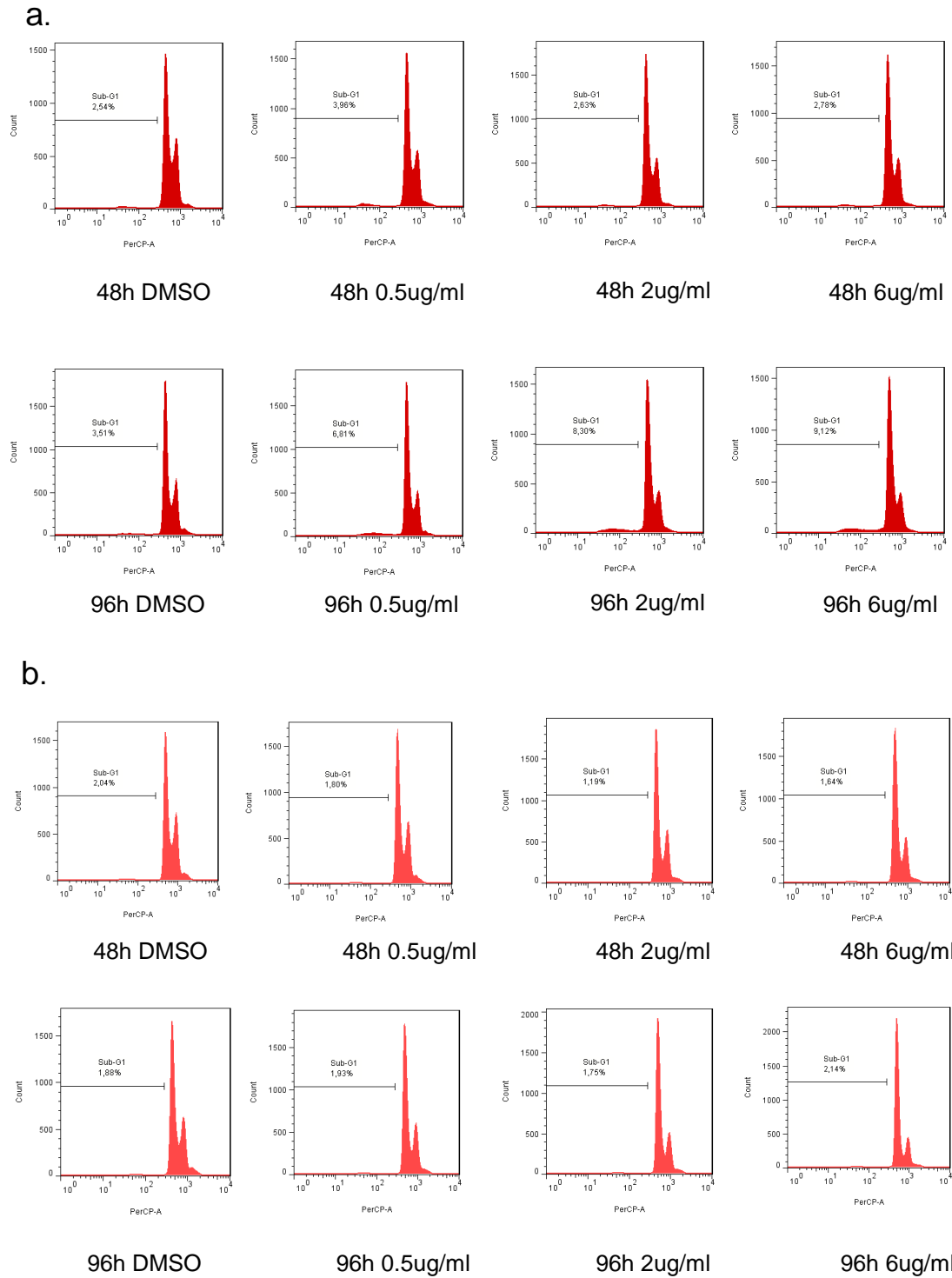


Figure.20 Cell cycle analysis on PDAC cell lines by AF treatment

(a) KP3 and (b) Panc-1 cells were treated with DMSO and AF (0.5µg/ml, 2µg/ml, 6µg/ml) for 48hrs and 96hrs. Cell cycle profile was investigated by PI staining. Percentage of Sub-G₁-phase population was calculated.

a.

48h	KP3 (%)			Panc-1 (%)		
Treatment ($\mu\text{g/ml}$)	G ₁ phase	S-phase	G ₂ /M phase	G ₁ phase	S-phase	G ₂ /M phase
DMSO	45.72	26.89	15.95	38.32	20.57	21.57
0.5	50.24	19.17	14.49	33.81	21.7	12.09
2	51.71	23.4	13.82	47.1	14.01	19.58
6	53	18.91	20.32	53.02	11.23	20.86

b.

96h	KP3 (%)			Panc-1 (%)		
Treatment ($\mu\text{g/ml}$)	G ₁ phase	S phase	G ₂ /M phase	G ₁ phase	S phase	G ₂ /M phase
DMSO	43.79	23.96	20.64	38.56	17.48	22.46
0.5	52.32	20.42	16.73	44.23	18.48	19.58
2	57.34	14.97	15.78	55.06	8.47	19.74
6	56.42	19.59	11.12	72.06	1.52	18.95

Table.1 Effect of AF treatment on KP3 and Panc-1 cell cycle distribution

a. 48hrs exposure to DMSO and AF (0.5 $\mu\text{g/ml}$, 2 $\mu\text{g/ml}$, 6 $\mu\text{g/ml}$). b. 96hrs exposure to DMSO and AF (0.5 $\mu\text{g/ml}$, 2 $\mu\text{g/ml}$, 6 $\mu\text{g/ml}$).

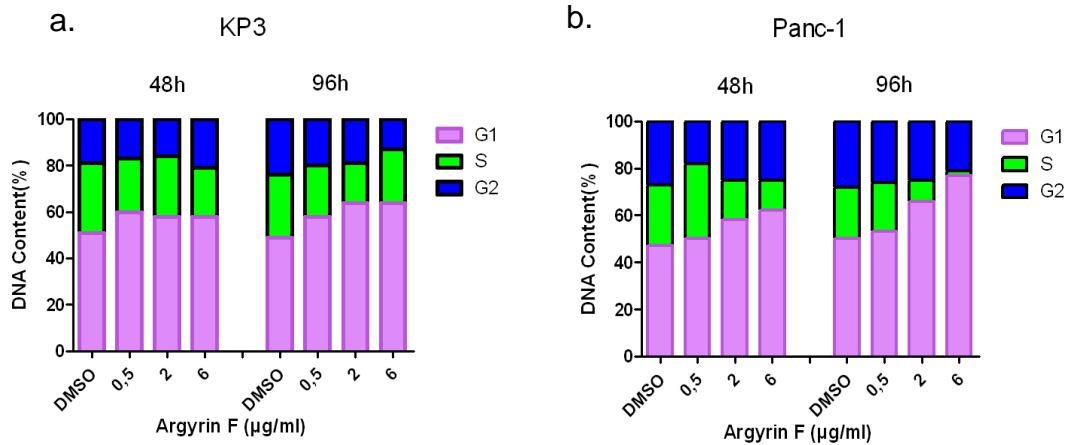


Figure.21 **AF treatment partially induces G₁/S phase cell cycle arrest in PDAC cell lines**

KP3 and Panc-1 cells were treated with DMSO and AF (0.5µg/ml, 2µg/ml, 6µg/ml) for 48hrs and 96hrs. Cell cycle profile was investigated by PI staining. a. Representative bar graph for KP3 cells; b. Representative bar graph for Panc-1 cells.

3.5 Both AF single and combinational (A+G) treatment inhibit tumor growth and prolong overall survival in KPC mice

To analyze the *in vivo* effect of AF we used a genetically engineered PDAC (KPC) mouse model, (Pdx1-Cre; Kras^{G12D}; p53^{Lox/+}). We subjected a total of 18 mice for survival analysis. Mice were treated intraperitoneally with AF (1mg/kg/body weight, Day1-Day3), combination of AF (1mg/kg/body weight Day1-Day3) + Gemcitabine (100mg/kg/body weight Day5) or vehicle starting at an age of 14-weeks as further mentioned in the Materials and Methods part.

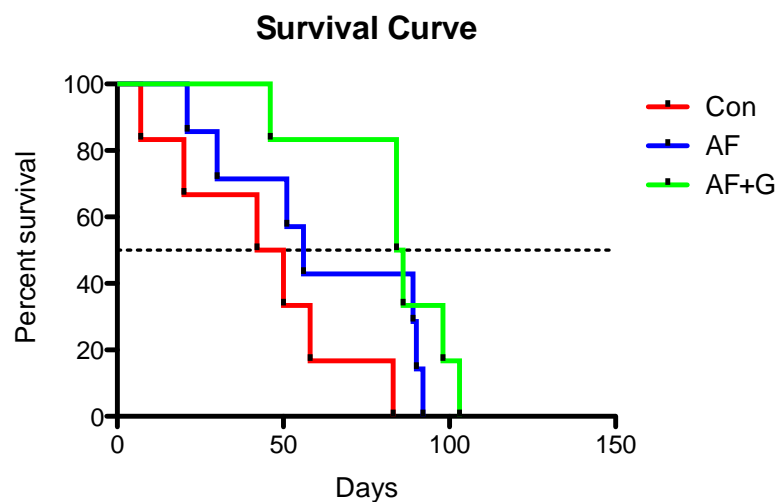
3.5.1 Survival experiment (tumor volume, body weight).

Mice were treated with AF single and (AF+G) combinational treatment starting at 14-weeks. The treatment outcome of AF single and (AF+ G) combinational treatment was compared to vehicle (PBS) therapy. AF+G combinational

treatment showed longest survival with a median of 85 days life span as compared to vehicle group ($p < 0.05$), which showed an average survival of only 46 days (Figure.22-a). Single treatment with AF also showed a longer survival with a median of 56 days as compared to the vehicle group (46 days), but there was no significant difference between both groups.

All mice were sacrificed at the end of this study when the critical illness was developed. As shown in Figure.22-b, AF single treatment and also in combination with G showed an effective reduction in tumor volume as compared to the vehicle group $p < 0.05$. Additionally, significant decrease in pancreatic tumor volume was also macroscopically observed under all treatment groups (AF single, AF+G) as compared to the vehicle group (Figure.22-c). Furthermore, the body weight of mice in all groups was measured during the study (Figure.22-d). Both AF and AF+G groups showed stable body weight throughout the experiment. Altogether, AF as a single agent as well as in combination with G was safe and without side effects.

a.



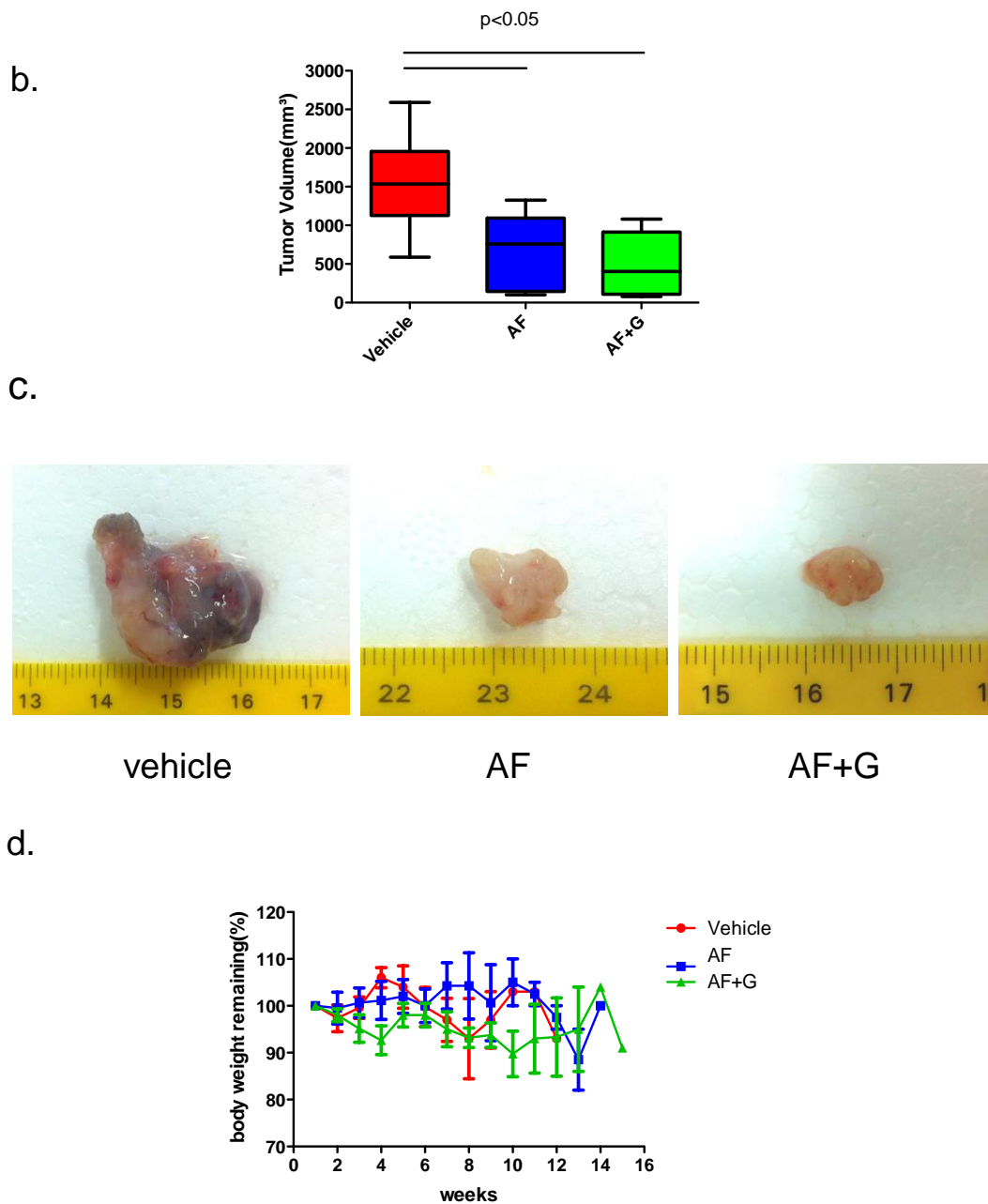


Figure.22 **AF+G combinational treatment prolongs survival lifespan in PDAC and resulted in the reduction of tumor volume.**

a. Survival is extended by the combination treatment of AF and G (median survival vehicle 46 days vs. 85 days with AF+G; $p < 0.05$ $n = 6$; vehicle [red], AF [blue], AF+G [green]). b. Quantification of tumor volume ($n = 6$) c. Represents macroscopic pictures of tumors from vehicle, AF and AF+G combinational treatment group. Tissues were harvested at the end of the experiment. d. The body weight of mice in all the groups was measured throughout the course of the experiment.

3.5.2 Analysis of metastasis incidence and tumor progression *in vivo*

The metastasis incidences were shown in Table.2, 100% (6/6) ascites and 66.7% (4/6) metastasis were observed in the vehicle group. In the AF group, ascites was observed in 66.7% (4/6) of mice and 16.7% (1/6) showed metastasis. In the combinational treatment group, 16.7% (1/6) had ascites and no metastasis were observed. The incidence of metastasis we observed included liver and peritoneum.

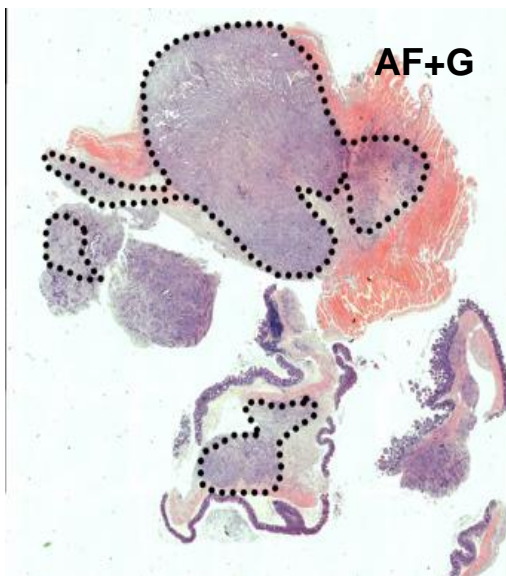
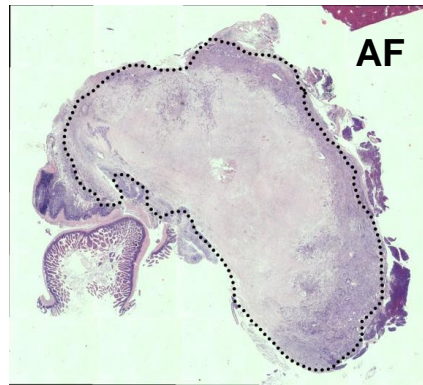
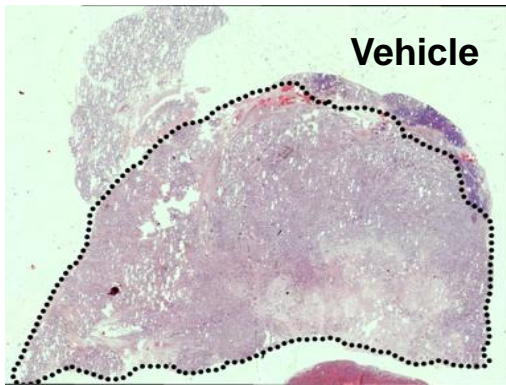
	Vehicle(n=6)	AF (n=6)	AF+G (n=6)
Incidence of metastasis	66.7%	16.7%	0%
Ascites	100%	66.7%	16.7%

Table.2 Metastasis incidence and ascites in KPC mice

Metastasis included liver metastasis and peritoneal metastasis in this study.

In order to elucidate the anti-tumor effect of AF single and AF+G combinational treatment on tumor progression, areas of PDAC were compared to the normal pancreatic tissue (Figure.23-a). We found that KPC mice treated with vehicle showed large PDACs without remaining normal pancreatic tissue (Figure.23). Mice treated by either AF or AF+G showed smaller PDAC (Figure.23-b). Thus, these results highlighted that AF single treatment or in combination with G effectively impair PDAC progression *in vivo*. Interestingly, we observed a significant amount of necrosis especially in the AF single treatment group (Figure.24). However, the combinational treatment (AF+G) did not result in different necrotic areas compared to the vehicle group.

a.



b.

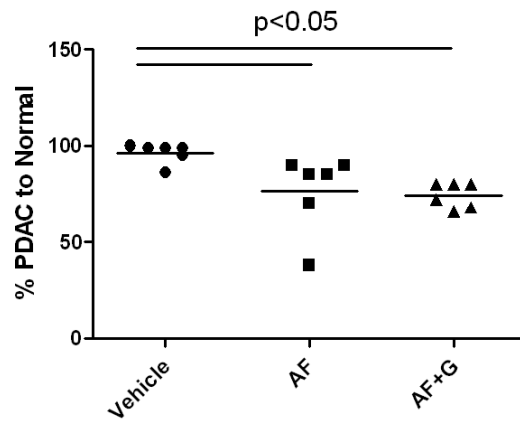


Figure.23 **AF and AF+G combinational treatment impaired PDAC progression in KPC mice**

a. Representative image of full tumors from vehicle, AF and AF+G combinational treatment groups. Dotted lines sketch out the tumor tissue, areas without lining represent normal pancreatic tissue. b. The graph illustrates the percentage of each pancreas occupied by the tumor in individual mice. Each symbol represents a mice and the horizontal line represents percentage of each group (n=6).

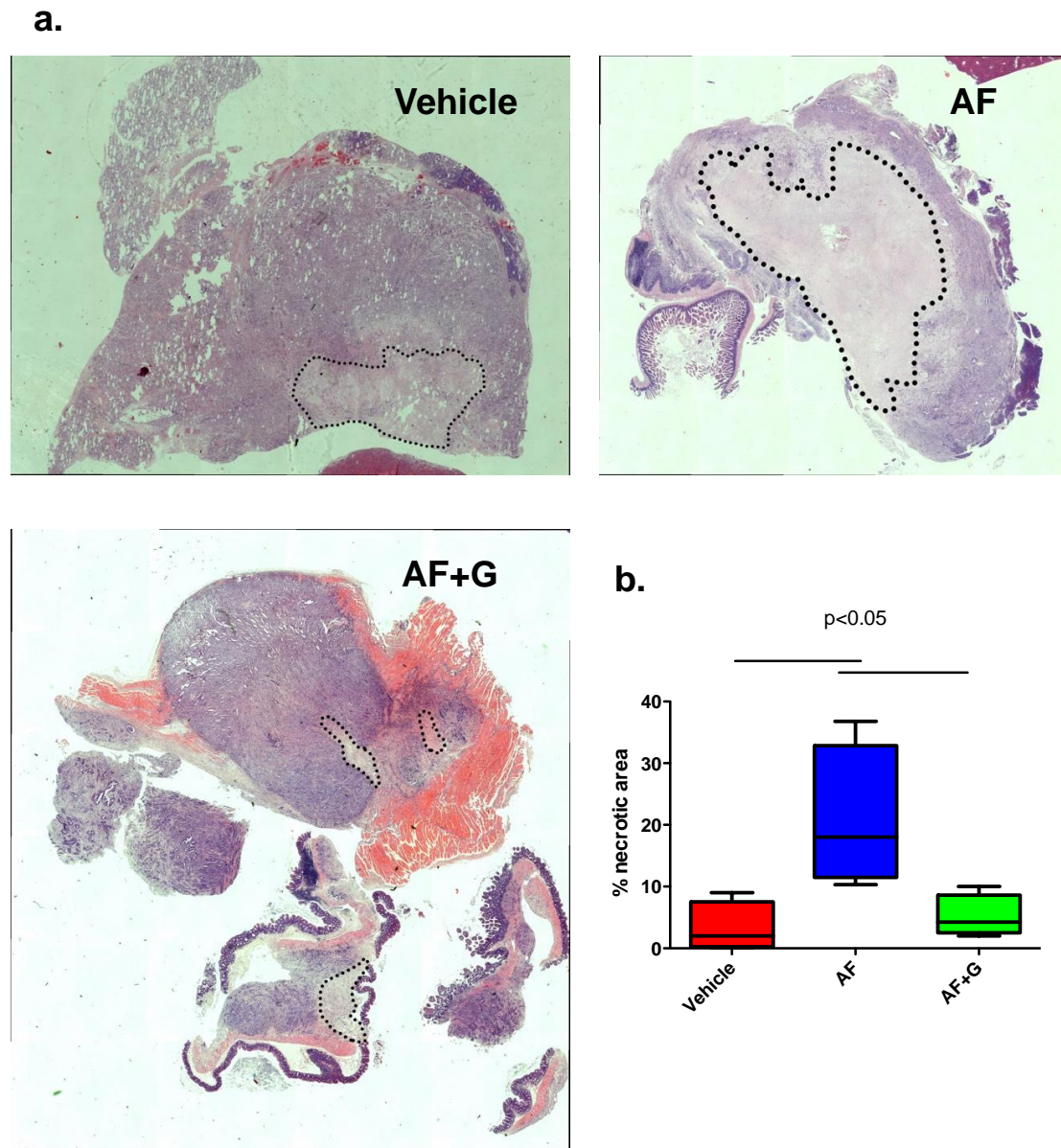


Figure.24 **AF single treatment showed more necrosis in the KPC mouse *in vivo***

a. Representative image of full tumors from vehicle, AF and AF+G combinational treatment groups. Dotted lines sketch out the necrotic area. b. Quantification of necrosis in the survival study. Differences were considered as statistically significant when the p-value was < 0.05.

3.5.3 Analysis of Ki-67 and CD34 expression in *in vivo* PDAC tumors

To analyze the *in vivo* drug treatment effect on cell proliferation, we performed Ki67 staining [55]. As shown in Figure.25, combinational treatment (AF+G)

resulted in an effective decrease of Ki-67 positive cells (5%) as compared to the vehicle group (16%) ($p < 0.05$). Although, AF single treatment showed a decrease in Ki-67 staining but the results were not significant in comparison to the vehicle group.

Angiogenesis is a proliferative process resulting in the development of new blood vessels from existing endothelial cells and occurs during reproduction, development and wound repair. Tumor angiogenesis is usually quantified as microvascular density (MVD). In the present study MVD was mainly assessed in highly vascularized tumor areas by using the pan-endothelial antibody, CD34 [56]. Many data has assumed that angiogenic activity is associated with the development and progression of some solid tumors and has an important prognostic value [57]. As shown in Figure.26, the MVD-CD34 score was significantly higher in the vehicle group in comparison to both AF single treatment and AF+G group ($p < 0.05$). However, no significant difference was observed between the two treatment groups (AF, AF+G).

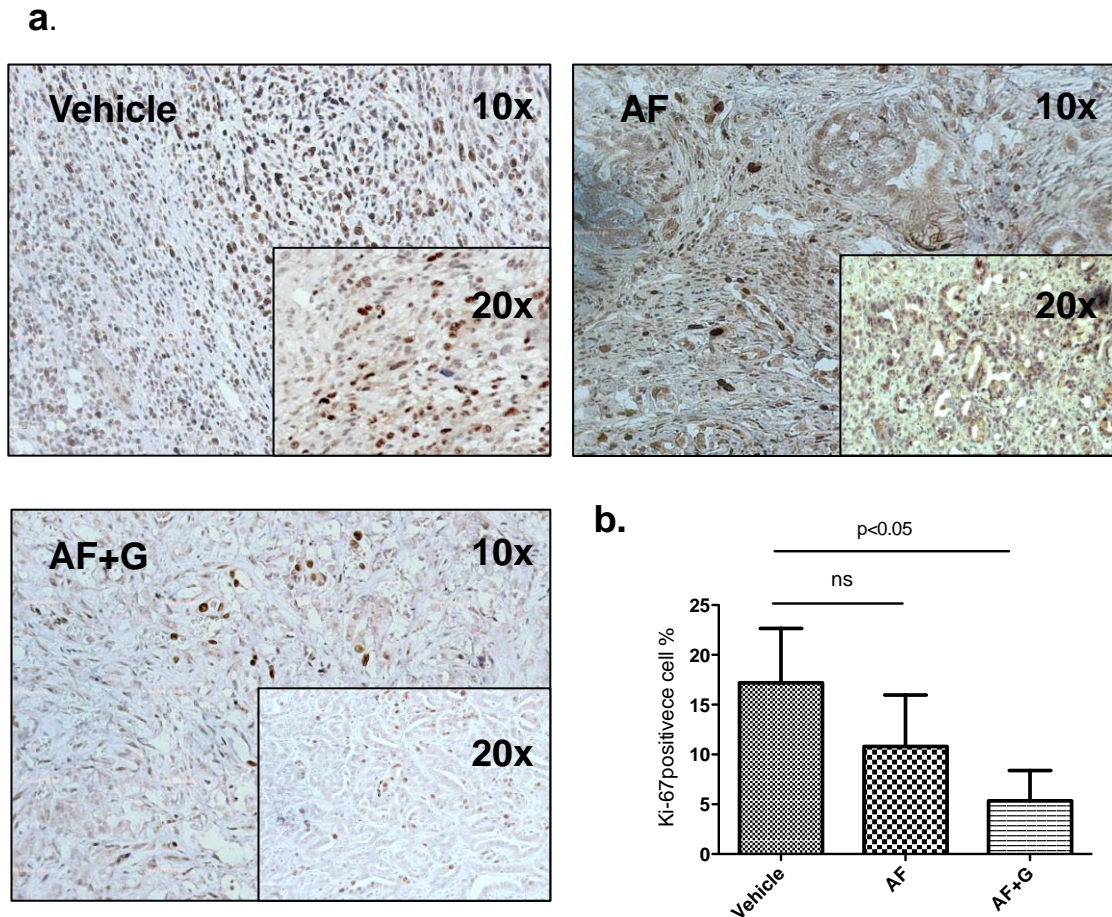


Figure.25 **AF+G combinational treatment resulted in an anti-proliferative effect on *in vivo* tumors.**

a. Ki67 staining of pancreatic tumors from each treatment group (n=6, 10x and 20x magnification). b. Quantification of Ki67 staining in the tumor tissues(n=6), showing reduction in Ki67 positive cells following AF+G combinational treatment. Differences were considered as statistically significant when the p-value was < 0.05 and ns when p-value was >0.05. The error bar represents standard deviation.

a.

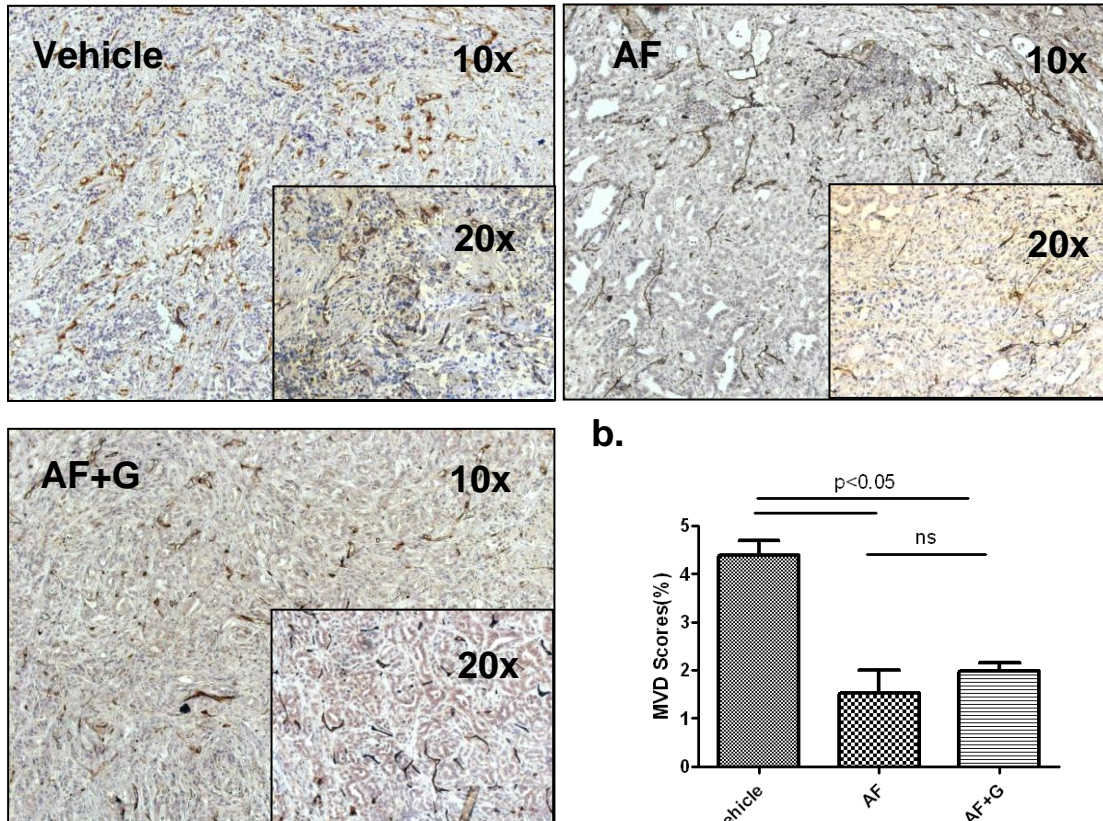


Figure.26 **AF+G combinational treatment inhibits the angiogenesis on *in vivo* tumors.**

a. Histological representative CD34 IHC-stained images for each group (vehicle, AF, AF+G, 10x and 20x magnification). b. Quantification of MVD scores were plotted in bar graph. Differences were considered as statistically significant when the p-value was < 0.05 and ns when p-value was >0.05. The error bar represents standard deviation.

4. Discussion

PDAC is an aggressive malignancy and currently the fourth leading cause of cancer related deaths in the US [58]. Although novel chemotherapies are available, there overall survival and the therapy response is still limited. In the quest for new targets for PDAC therapy, the proteasome and its inhibitors have been the focus of academic and industrial research [59]. Proteasome inhibitors have anti-cancer activity through a variety of cellular mechanisms, including anti-proliferative activity, induction of apoptosis, interference with cell-cycle progression, inhibition of angiogenesis, etc. In the present study, we study the new proteasome inhibitor Argyrin F (AF), which has been identified as a promising antitumor compound through its p27^{kip1} stabilization effect [52], on PDAC carcinogenesis.

In vitro, we selected two human PDAC cell lines: KP3 and Panc-1 due to preliminary IC₅₀ experiment under AF treatments. These two cell lines are from different origins: Panc-1 is a common available human PDAC cell line, cultured from a primary tumor without evidence of metastasis, in contrast KP3 is obtained from liver metastasis of a human pancreatic tumor. We found effective inhibition of cell proliferation in both Panc-1 and KP3 cells compared to their DMSO controls. However, Panc-1 cells demonstrated to be more sensitive to AF treatment after 96h compared to KP3 cells. Nিকেleit et al. [51] have revealed the mechanism by which Argyrin A (the analogue of AF) influences tumor cell proliferation all depending on stabilization of p27^{kip1} and Zhang et al. [60] showed that up-regulating the expression of p21^{waf1/cip1} has an inhibitory effect on cell proliferation of Panc-1. Next, Bülow et al. [52] has shown that treatment with AF resulted in a dose-dependent expression of p27^{kip1} in SW-480 colon carcinoma cells.

In our study, we also observed a relative up-regulation of p27^{kip1} and p21^{waf1/cip1} expression in a time-dose-dependent manner under AF treatment for both cell lines by Western Blot. It is known that p27^{kip1} is one the most frequently deregulated tumor suppressor proteins in human cancers [46]. Decreased p27^{kip1} levels have been correlated with tumor aggressiveness and poor patient survival [46];[48];[61]. Sarker et al. [62] reported that an oncogenic miRNA which targets p27^{kip1} can consequently up-regulate the expression of p27^{kip1}, leading to the inhibition of cell proliferation and migration of PDAC cell lines (MiaPaCa-2, Panc-1 and BxPC3). Yadav et al. [63] reported that Gatifloxacin can induce p21^{waf1/cip1} and p27^{kip1} levels in PDAC cell lines (Panc-1, MiaPaCa-2) by causing S-phase arrest to perform its anti-tumor effect. Zhang et al. [64] and Katayose et al. [65] have revealed that p27^{kip1} expression can also be correlated to the induction of apoptosis, but the exact mechanism of this correlation is not yet identified.

As it was observed in the present study, KP3 cells demonstrated a gradually increased population of sub-G₁-phase cells after 96hrs under AF treatment. This is consistent with the result that AF treatment also induced a considerable apoptosis on KP3 cell lines as compared to Panc-1 cells (96h: 34% vs 16%), which are in line with the p27^{kip1} expression levels and cell cycle profile. Importantly, not all tumor cells that were treated with AF *in vitro* underwent a considerable apoptosis; some instead underwent cell-cycle arrest. We found that AF treatment might exert the cytostatic effect on Panc-1 cells by arresting the cells in the G₁/S-phase of the cell cycle profile, but KP3 cells did not show any cell cycle arrest under AF treatment. These results indicate that anti-proliferative effect of AF might behave differently on Panc-1 and KP3: Panc-1 mainly underwent cell-cycle arrest and KP3 mainly induced cell apoptosis.

Since we observed an up-regulation of p21^{waf1/cip1} and p27^{kip1} expression under AF treatment and p21^{waf1/cip1} is known as a senescence mediator of the death receptor, we next performed X-gal staining to investigate whether AF induces cell senescence in addition to apoptosis. Cellular senescence is defined as an irreversible form of cell cycle arrest. Campisi et al. [66] pointed out that two cell-cycle inhibitors that are often expressed by senescent cells are the cyclin-dependent kinase inhibitors: p21^{waf1/cip1} and p16^{INK4a}. Park et al. [67] proved that all-trans retinoic acid can induce cellular senescence via upregulation of p16^{INK4a}, p21^{waf1/cip1} and p27^{kip1}, as the cyclin-dependent kinase inhibitors, resulting in a cell cycle arrest in G₁-phase. Unfortunately, we could not correlate the expression level of p21^{waf1/cip1} and p27^{kip1} with the induction of senescence in our tested cell lines. Both of our cell lines failed to show high induction of senescence in contrary to the immunoblots showing considerable upregulation of both the markers (p21^{waf1/cip1} and p27^{kip1}). This might indicate that AF treatment mainly induces apoptosis and less senescence, but additional experiments are required in order to confirm the ultimate cell death mechanism induced upon AF treatment.

In the recent years, accumulated evidence has suggested that EMT plays a critical role for PDAC development associated with invasion, migration, early metastasis and chemo-resistance [42]. Moreover, EMT has been demonstrated in human PDAC specimens, and tumorigenic cells with mesenchymal features to show a positive correlation with high-grade PDAC [68]. Specifically, PDAC with more mesenchymal features resulted in a worse survival and increased numbers of metastasis. We analyzed two EMT-markers in the present study: E-cadherin and N-cadherin. E-cadherin is expressed in epithelial cells, and its expression is decreased during EMT process in embryonic development, tissue fibrosis, and cancer. Moreover, loss of

E-cadherin function promotes EMT and is associated with advanced PDAC [69];[70]. N-cadherin is down regulated at other sites of EMT, including the neural crest and somites. N-cadherin used to monitor the progress of EMT during embryonic development and cancer progression [42]. We found that AF treatment resulted in an *in vitro* inhibition of migration and invasion in PDAC cells. For Panc-1 cells we observed a time-dose-dependent decrease of mesenchymal marker (N-cadherin) and increase of epithelial marker (E-cadherin). On the other hand, the EMT markers were unchanged for KP3 cells. Since we do not see any change in EMT expression in KP3 cells after AF treatment this might correlate with the different background of the two tested cell lines. Panc-1 cells after AF treatment show relatively effective inhibition of mesenchymal markers and also of invasion and migration. This explains that AF influences EMT process in Panc-1 cells but not much for KP3 cells. The difference in drug efficacy regarding EMT can be attributed to various reasons like different metastasis backgrounds of the cell lines which might impact differently to the ultimate effectiveness of the drug. Taken together, these results suggest that AF treatment selectively inhibits EMT in PDAC cells.

For the *in vivo* part of our study, we used a well-established (KPC) mouse model: Pdx1-Cre; LSL-Kras^{G12D/+}; p53^{Lox/+} which recapitulate human PDAC progression [53]; [71]. KPC mouse has a dramatically shortened median survival of approximately 5 months and it starts to develop advanced PDAC from 2 to 3 months onwards. Moreover, the natural microenvironment of the pancreas is maintained in this mouse model [53]. In our study we commenced the treatment at 14 weeks of age, at this timepoint KPC mice have precursor lesions and already show small PDAC formation [53]. Most significantly, AF in combination with G significantly inhibited pancreatic carcinogenesis in KPC mice. AF and AF+G treated animals significantly reduced incidence of

metastasis and the treatment regime was well tolerated in all experimental groups. This study also demonstrated that AF+G combinational treatment showed significant anti-proliferative effect as seen by reduced Ki-67 expression in PDAC tumors.

It is known that angiogenic activity is associated with the development and progression of PDAC and has an important prognostic value [57]. Hiroshima, et al. [72] showed that tumor-targeting *Salmonella typhimurium* A1-R in combination with anti-angiogenesis therapy (Bevacizumab + G) can reduce the xenograft tumor volume. In addition, Huang et al. [73] showed that Embelin inhibiting Akt and Sonic hedgehog pathway can inhibit pancreatic tumor growth by regulating angiogenesis and metastasis. Controversially, some research groups showed that PDAC is hypovascular in both humans and KPC mice, so tumor progression is thought to thrive without the requirement for excessive angiogenesis [74]. Suzuki et al. [75] demonstrated that combination of NF- κ B inhibitor and G can exert anti-tumor effects by inhibiting angiogenesis. In the present study, our results showed a reduction of tumor volume as well as the MVD (micro vessel density) score under AF and AF+G combinational treatment. These results relate to the study of Bülow L et al. [52] and showed that AF leads to a faster destruction of blood vessels than Argyrin A. Our results indicate that the combinational treatment of AF+G can inhibit the tumor growth by regulating angiogenesis and this might be a potential down staging approach for patients with unresectable lesion due to a smaller tumor volume. Moreover, we observed a significant amount of necrosis only in the AF single treatment group, but not in the combinational treatment group. Unlike tumor core necrosis, which is commonly observed in xenograft tumors, in KPC tumors combinational treatment induced necrosis that occurred in patches scattered throughout the tumor. In the present study, we found no correlation

between final tumor volume and necrosis or treatment length and necrosis, Cook et al. also showed similar results in KPC mouse model treated by gamma secretase inhibitor and gemcitabine [76].

The scarcity of endothelial fenestrations and open interendothelial junctions in treatment-naive KPC tumors stands in contrast to observations in xenografts, allografts and some spontaneous tumor models [77]. Some ultrastructural changes may permit access to therapeutic agents [78], their absence may contribute towards delivery inefficiency in the KPC tumors and explain the differential chemotherapeutic sensitivities between spontaneous tumors and other models. According to Olive et al. [71], KPC mice demonstrate innate resistance to G, so they suggest that inhibition of Hedgehog signaling can enhance delivery of G in KPC mice. Consistent with this study, combination of *nab*-paclitaxel and gemcitabine can also improve G delivery to pancreatic tumor showing an increased intratumoral level of G [79]. In the present study, AF+G combinational treatment resulted in a longer median survival and smaller tumor volume as well as reduced tumor cell proliferation, it indicates that AF might enhance Gemcitabine drug delivery in KPC mice.

In conclusion, our findings indicated that AF treatment resulted in an inhibition of cell proliferation, migration, invasion and colony formation in PDAC cell lines. AF therapy induced a considerable amount of apoptosis and partially senescence in the tested PDAC cell lines in a dose-time-dependent manner. AF induced a gradually increasing population of cells in sub-G1-phase for KP3 cells and also resulted in a G₁/S-phase arrest on Panc-1 cells. AF treatment showed considerable inhibition of EMT in Panc-1 cells but not in KP3 cells. Most importantly, combinational treatment by AF+G showed prolonged survival and caused significant tumor reduction by inhibiting tumor cell

proliferation and angiogenesis. Taken together, AF in combination with G might be a new and promising therapeutic approach for patients with PDAC. but further studies are needed to validate our experimental findings.

5. Summary

PDAC is the fourth most common cause of cancer death in the US and Europe. Current systemic chemotherapies are limited and new drugs are needed to improve survival. In the present study, we have analyzed *in vitro* (KP3, Panc-1) and *in vivo* (Pdx1-Cre; LSL-Kras^{G12D}; p53^{lox/+}) the antitumor effect of the proteasome inhibitor Argyrin F (AF) single and in combination with Gemcitabine (AF+G). *In vitro*, AF therapy induced a dose-and time-dependent growth inhibition of KP3 and Panc-1 cells. Moreover, AF treatment resulted in an inhibition of migration, invasion and colony formation in PDAC cell lines. AF therapy induced a considerable amount of apoptosis and partially senescence in the tested PDAC cell lines in a dose-and time-dependent manner. Furthermore, cell cycle profile analysis showed that AF induced a gradually increasing population of cells in sub-G₁-phase for KP3 cells and also resulted in a G₁/S-phase arrest on Panc-1 cell. AF treatment showed considerable inhibition of EMT in Panc-1 cells but not in KP3 cells. *In vivo*, most importantly, combinational treatment by AF+G showed prolonged survival and caused significant tumor reduction. Less incidences of metastasis and ascites was observed after AF single and AF+G treatment. Expression of both the markers ki67 and CD34 showed reduced expression in the treatment groups (AF, AF+G). AF and AF+G treatment regimes were well tolerated by all the animals used in the study. In conclusion, our work demonstrates that treatment with AF can successfully inhibit the growth of PDAC *in vitro* and *in vivo*. Especially, AF in combination with G might be a new and promising therapeutic approach for patients with PDAC, but further studies are needed to validate our findings.

6. Zusammenfassung

Das Pankreaskarzinom (PDAC) gehört in den USA und Europa zu der vierthäufigsten Ursache an einem Malignom zu versterben. Aktuelle systemische Chemotherapien sind limitiert und es werden dringend neue Substanzen gesucht um das Überleben zu verbessern. In der vorliegenden Arbeit haben wir *in vitro* (KP3, Panc-1) und *in vivo* (Pdx1-Cre; LSL-Kras^{G12D}; p53^{lox/+}) die anti-tumoröse Eigenschaft des Proteasom-Inhibitors Argyrin F (AF) als Monotherapie und in Kombination mit Gemcitabine (AF+G) untersucht. *In vitro* konnte die AF Therapie eine Dosis- und Zeit-abhängige Inhibition von KP3 und Panc-1 Zellen erreichen. Außerdem führte die AF Therapie zu einer Inhibition der Migration, Invasion und Kolonie-Formation. Ferner induzierte die AF Applikation einen Dosis- und Zeit-abhängigen Zelltod und führte zur Senescence. Die Analyse des Zellzyklus-Profiles ergab unter Therapie für KP3 Zellen eine erhöhte Population in der Sub-G₁-Fraktion und für Panc-1 Zellen in der G₁/S-Fraktion. AF führte dabei nur zu einer Inhibition der epithelialen mesenchymalen Transition (EMT) bei den Panc-1 Zellen. *In vivo*, erzielte die Kombinationstherapie (AF+G) ein verlängertes Überleben und erreichte eine signifikante Tumorverkleinerung. Sowohl AF als auch AF+G führten zu einer Abnahme von Aszites und Metastasen. Auch die Expression von Ki67 und CD34 konnten mit der Mono- und Kombinationstherapie reduziert werden. Alle Therapieregime waren im Mausmodell gut verträglich. Wir konnten somit erfolgreich demonstrieren, dass eine Therapie mit AF *in vitro* und *in vivo* das Wachstum von PDAC Zellen inhibieren kann. Vor allem die Kombination AF+G könnte somit eine neue und erfolgsversprechend Therapiemöglichkeit für Patienten mit PDAC darstellen, aber weitere Studien sind erforderlich um unsere Ergebnisse zu validieren.

7. References List

1. Raimondi, S., P. Maisonneuve, and A.B. Lowenfels, *Epidemiology of pancreatic cancer: an overview*. *Nat Rev Gastroenterol Hepatol*, 2009. **6**(12): p. 699-708.
2. Hurton, S., et al., *The current state of pancreatic cancer in Canada: incidence, mortality, and surgical therapy*. *Pancreas*, 2014. **43**(6): p. 879-85.
3. Zavoral, M., et al., *Molecular biology of pancreatic cancer*. *World J Gastroenterol*, 2011. **17**(24): p. 2897-908.
4. Vincent, A., et al., *Pancreatic cancer*. *Lancet*, 2011. **378**(9791): p. 607-20.
5. He, Y., et al., *Pancreatic cancer incidence and mortality patterns in China, 2011*. *Chin J Cancer Res*, 2015. **27**(1): p. 29-37.
6. Bachmann, J., et al., *Cachexia worsens prognosis in patients with resectable pancreatic cancer*. *J Gastrointest Surg*, 2008. **12**(7): p. 1193-201.
7. Conroy, T., et al., *FOLFIRINOX versus gemcitabine for metastatic pancreatic cancer*. *N Engl J Med*, 2011. **364**(19): p. 1817-25.
8. Sohal, D.P., et al., *Predicting early mortality in resectable pancreatic adenocarcinoma: A cohort study*. *Cancer*, 2015. **121**(11): p. 1779-84.
9. Schulte, A., et al., *Cigarette smoking and pancreatic cancer risk: More to the story than just pack-years*. *European Journal of Cancer*, 2014. **50**(5): p. 997-1003.
10. Zou, L., et al., *Non-linear dose–response relationship between cigarette smoking and pancreatic cancer risk: Evidence from a meta-analysis of 42 observational studies*. *European Journal of Cancer*, 2014. **50**(1): p. 193-203.
11. Jang, J.H., et al., *Interaction of polymorphisms in mitotic regulator genes with cigarette smoking and pancreatic cancer risk*. *Mol Carcinog*, 2013. **52 Suppl 1**: p. E103-9.
12. McAuliffe, J.C. and J.D. Christein, *Type 2 diabetes mellitus and pancreatic cancer*. *Surg Clin North Am*, 2013. **93**(3): p. 619-27.
13. Stevens, R.J., A.W. Roddam, and V. Beral, *Pancreatic cancer in type 1 and young-onset diabetes: systematic review and meta-analysis*. *Br J Cancer*, 2007. **96**(3): p. 507-9.
14. Austin, M.A., et al., *Family history of diabetes and pancreatic cancer as risk factors for pancreatic cancer: the PACIFIC study*. *Cancer Epidemiol Biomarkers Prev*, 2013. **22**(10): p. 1913-7.

15. Berrington de Gonzalez, A., S. Sweetland, and E. Spencer, *A meta-analysis of obesity and the risk of pancreatic cancer*. Br J Cancer, 2003. **89**(3): p. 519-23.
16. Biankin, A.V., et al., *Pancreatic cancer genomes reveal aberrations in axon guidance pathway genes*. Nature, 2012. **491**(7424): p. 399-405.
17. Raimondi, S., et al., *Pancreatic cancer in chronic pancreatitis; aetiology, incidence, and early detection*. Best Pract Res Clin Gastroenterol, 2010. **24**(3): p. 349-58.
18. Amundadottir, L., et al., *Genome-wide association study identifies variants in the ABO locus associated with susceptibility to pancreatic cancer*. Nat Genet, 2009. **41**(9): p. 986-90.
19. Wolpin, B.M. and M.J. Stampfer, *Defining determinants of pancreatic cancer risk: are we making progress?* J Natl Cancer Inst, 2009. **101**(14): p. 972-3.
20. Ojajarvi, I.A., et al., *Occupational exposures and pancreatic cancer: a meta-analysis*. Occup Environ Med, 2000. **57**(5): p. 316-24.
21. Li, H.Y., et al., *Pancreatic cancer: diagnosis and treatments*. Tumour Biol, 2015. **36**(3): p. 1375-84.
22. Lee, E.S. and J.M. Lee, *Imaging diagnosis of pancreatic cancer: a state-of-the-art review*. World J Gastroenterol, 2014. **20**(24): p. 7864-77.
23. de la Santa, L.G., et al., *Radiology of pancreatic neoplasms: An update*. World J Gastrointest Oncol, 2014. **6**(9): p. 330-43.
24. Maithel, S.K., et al., *Preoperative CA 19-9 and the yield of staging laparoscopy in patients with radiographically resectable pancreatic adenocarcinoma*. Ann Surg Oncol, 2008. **15**(12): p. 3512-20.
25. Wagner, M., et al., *Curative resection is the single most important factor determining outcome in patients with pancreatic adenocarcinoma*. Br J Surg, 2004. **91**(5): p. 586-94.
26. Li, D., et al., *Pancreatic cancer*. Lancet, 2004. **363**(9414): p. 1049-57.
27. Burris, H.A., 3rd, et al., *Improvements in survival and clinical benefit with gemcitabine as first-line therapy for patients with advanced pancreas cancer: a randomized trial*. J Clin Oncol, 1997. **15**(6): p. 2403-13.
28. Renouf, D.J., et al., *A phase II study of erlotinib in gemcitabine refractory advanced pancreatic cancer*. Eur J Cancer, 2014. **50**(11): p. 1909-15.
29. Goldstein, D., et al., *nab-Paclitaxel plus gemcitabine for metastatic pancreatic cancer: long-term survival from a phase III trial*. J Natl Cancer Inst, 2015. **107**(2).

30. Tanaka, M., et al., *International consensus guidelines 2012 for the management of IPMN and MCN of the pancreas*. Pancreatology, 2012. **12**(3): p. 183-197.
31. Klapman, J. and M.P. Malafa, *Early detection of pancreatic cancer: why, who, and how to screen*. Cancer Control, 2008. **15**(4): p. 280-7.
32. Hingorani, S.R., et al., *Preinvasive and invasive ductal pancreatic cancer and its early detection in the mouse*. Cancer Cell, 2003. **4**(6): p. 437-50.
33. Rustgi, A.K., *The molecular pathogenesis of pancreatic cancer: clarifying a complex circuitry*. Genes Dev, 2006. **20**(22): p. 3049-53.
34. Sipos, B., et al., *Pancreatic intraepithelial neoplasia revisited and updated*. Pancreatology, 2009. **9**(1-2): p. 45-54.
35. Zamboni, G., et al., *Precancerous lesions of the pancreas*. Best Pract Res Clin Gastroenterol, 2013. **27**(2): p. 299-322.
36. Kanda, M., et al., *Presence of somatic mutations in most early-stage pancreatic intraepithelial neoplasia*. Gastroenterology, 2012. **142**(4): p. 730-733.e9.
37. Campbell, S.L., et al., *Increasing complexity of Ras signaling*. Oncogene, 1998. **17**(11 Reviews): p. 1395-413.
38. Klimstra, D.S. and D.S. Longnecker, *K-ras mutations in pancreatic ductal proliferative lesions*. Am J Pathol, 1994. **145**(6): p. 1547-50.
39. Ji, B., et al., *Ras activity levels control the development of pancreatic diseases*. Gastroenterology, 2009. **137**(3): p. 1072-82, 1082.e1-6.
40. Furukawa, T., M. Sunamura, and A. Horii, *Molecular mechanisms of pancreatic carcinogenesis*. Cancer Sci, 2006. **97**(1): p. 1-7.
41. Welsch, T., J. Kleeff, and H. Friess, *Molecular pathogenesis of pancreatic cancer: advances and challenges*. Curr Mol Med, 2007. **7**(5): p. 504-21.
42. Thiery, J.P., *Epithelial-mesenchymal transitions in tumour progression*. Nat Rev Cancer, 2002. **2**(6): p. 442-54.
43. Cano, C.E., Y. Motoo, and J.L. Iovanna, *Epithelial-to-mesenchymal transition in pancreatic adenocarcinoma*. ScientificWorldJournal, 2010. **10**: p. 1947-57.
44. Beuran, M., et al., *The epithelial to mesenchymal transition in pancreatic cancer: A systematic review*. Pancreatology, 2015. **15**(3): p. 217-25.
45. Polyak, K., et al., *Cloning of p27Kip1, a cyclin-dependent kinase inhibitor and a potential mediator of extracellular antimitogenic signals*. Cell, 1994. **78**(1): p. 59-66.
46. Lloyd, R.V., et al., *p27kip1: A Multifunctional Cyclin-Dependent Kinase Inhibitor with Prognostic Significance in Human Cancers*. The American Journal of Pathology, 1999. **154**(2): p. 313-323.

47. Juuti, A., et al., *Loss of p27 expression is associated with poor prognosis in stage I-II pancreatic cancer*. *Oncology*, 2003. **65**(4): p. 371-7.
48. Lu, C.D., et al., *Loss of p27Kip1 expression independently predicts poor prognosis for patients with resectable pancreatic adenocarcinoma*. *Cancer*, 1999. **85**(6): p. 1250-60.
49. Abukhdeir, A.M. and B.H. Park, *p21 and p27: roles in carcinogenesis and drug resistance*. *Expert Reviews in Molecular Medicine*, 2008. **10**: p. null-null.
50. Span, P.N., P.H. de Mulder, and F.C. Sweep, *Re: p27(Kip1) and cyclin E expression and breast cancer survival after treatment with adjuvant chemotherapy*. *J Natl Cancer Inst*, 2007. **99**(9): p. 738.
51. Nিকেলেইট, I., et al., *Argyirin a reveals a critical role for the tumor suppressor protein p27(kip1) in mediating antitumor activities in response to proteasome inhibition*. *Cancer Cell*, 2008. **14**(1): p. 23-35.
52. Bulow, L., et al., *Synthesis and biological characterization of argyirin F*. *ChemMedChem*, 2010. **5**(6): p. 832-6.
53. Hingorani, S.R., et al., *Trp53R172H and KrasG12D cooperate to promote chromosomal instability and widely metastatic pancreatic ductal adenocarcinoma in mice*. *Cancer Cell*, 2005. **7**(5): p. 469-83.
54. Campisi, J. and F. d'Adda di Fagagna, *Cellular senescence: when bad things happen to good cells*. *Nat Rev Mol Cell Biol*, 2007. **8**(9): p. 729-40.
55. Lee, C., et al., *Elevated expression of tumor miR-222 in pancreatic cancer is associated with Ki67 and poor prognosis*. *Med Oncol*, 2013. **30**(4): p. 700.
56. Wang, W.Q., et al., *Intratumoral alpha-SMA enhances the prognostic potency of CD34 associated with maintenance of microvessel integrity in hepatocellular carcinoma and pancreatic cancer*. *PLoS One*, 2013. **8**(8): p. e71189.
57. Folkman, J., et al., *Induction of angiogenesis during the transition from hyperplasia to neoplasia*. *Nature*, 1989. **339**(6219): p. 58-61.
58. Siegel, R., D. Naishadham, and A. Jemal, *Cancer statistics for Hispanics/Latinos, 2012*. *CA Cancer J Clin*, 2012. **62**(5): p. 283-98.
59. Gong, L., et al., *Bortezomib-induced apoptosis in cultured pancreatic cancer cells is associated with ceramide production*. *Cancer Chemother Pharmacol*, 2014. **73**(1): p. 69-77.
60. Zhang, Z., et al., *Up-regulation of p21WAF1/CIP1 by small activating RNA inhibits the in vitro and in vivo growth of pancreatic cancer cells*. *Tumori*, 2012. **98**(6): p. 804-11.

61. Porter, P.L., et al., *Expression of cell-cycle regulators p27Kip1 and cyclin E, alone and in combination, correlate with survival in young breast cancer patients.* Nat Med, 1997. **3**(2): p. 222-5.
62. Sarkar, S., et al., *Down-regulation of miR-221 inhibits proliferation of pancreatic cancer cells through up-regulation of PTEN, p27(kip1), p57(kip2), and PUMA.* Am J Cancer Res, 2013. **3**(5): p. 465-77.
63. Yadav, V., et al., *Gatifloxacin induces S and G2-phase cell cycle arrest in pancreatic cancer cells via p21/p27/p53.* PLoS One, 2012. **7**(10): p. e47796.
64. Zhang, Q., et al., *Inducible expression of a degradation-resistant form of p27Kip1 causes growth arrest and apoptosis in breast cancer cells.* FEBS Lett, 2005. **579**(18): p. 3932-40.
65. Katayose, Y., et al., *Promoting apoptosis: a novel activity associated with the cyclin-dependent kinase inhibitor p27.* Cancer Res, 1997. **57**(24): p. 5441-5.
66. Campisi, J., *Cellular senescence as a tumor-suppressor mechanism.* Trends Cell Biol, 2001. **11**(11): p. S27-31.
67. Park, S.H., J.S. Lim, and K.L. Jang, *All-trans retinoic acid induces cellular senescence via upregulation of p16, p21, and p27.* Cancer Lett, 2011. **310**(2): p. 232-9.
68. Rasheed, Z.A., et al., *Prognostic significance of tumorigenic cells with mesenchymal features in pancreatic adenocarcinoma.* J Natl Cancer Inst, 2010. **102**(5): p. 340-51.
69. Joo, Y.E., et al., *Expression of E-cadherin, alpha- and beta-catenins in patients with pancreatic adenocarcinoma.* Pancreatology, 2002. **2**(2): p. 129-37.
70. Hong, S.M., et al., *Loss of E-cadherin expression and outcome among patients with resectable pancreatic adenocarcinomas.* Mod Pathol, 2011. **24**(9): p. 1237-47.
71. Olive, K.P., et al., *Inhibition of Hedgehog signaling enhances delivery of chemotherapy in a mouse model of pancreatic cancer.* Science, 2009. **324**(5933): p. 1457-61.
72. Hiroshima, Y., et al., *Efficacy of tumor-targeting Salmonella typhimurium A1-R in combination with anti-angiogenesis therapy on a pancreatic cancer patient-derived orthotopic xenograft (PDOX) and cell line mouse models.* Oncotarget, 2014. **5**(23): p. 12346-57.
73. Huang, M., et al., *Embelin suppresses growth of human pancreatic cancer xenografts, and pancreatic cancer cells isolated from KrasG12D mice by inhibiting Akt and Sonic hedgehog pathways.* PLoS One, 2014. **9**(4): p. e92161.
74. Feig, C., et al., *The pancreas cancer microenvironment.* Clin Cancer Res, 2012. **18**(16): p. 4266-76.

75. Suzuki, K., et al., *Combined effect of dehydroxymethylepoxyquinomicin and gemcitabine in a mouse model of liver metastasis of pancreatic cancer*. Clin Exp Metastasis, 2013. **30**(4): p. 381-92.
76. Cook, N., et al., *Gamma secretase inhibition promotes hypoxic necrosis in mouse pancreatic ductal adenocarcinoma*. J Exp Med, 2012. **209**(3): p. 437-44.
77. Jacobetz, M.A., et al., *Hyaluronan impairs vascular function and drug delivery in a mouse model of pancreatic cancer*. Gut, 2013. **62**(1): p. 112-20.
78. Hashizume, H., et al., *Openings between defective endothelial cells explain tumor vessel leakiness*. Am J Pathol, 2000. **156**(4): p. 1363-80.
79. Frese, K.K., et al., *nab-Paclitaxel potentiates gemcitabine activity by reducing cytidine deaminase levels in a mouse model of pancreatic cancer*. Cancer Discov, 2012. **2**(3): p. 260-9.

8. Declaration

I hereby declare that all the experiments from the thesis were performed by myself under the supervision of Prof. Dr. med Ruben R. Plentz. This thesis is not published anywhere before.

Date:

Signature:

9. List of Publications

1. Wutka A¹, Palagani V¹, Barat S¹, **Chen X**¹, El Khatib M¹, Götze J¹, Belahmer H¹, Zender S², Bozko P¹, Malek NP¹, Plentz RR¹

“Capsaicin treatment attenuates cholangiocarcinoma carcinogenesis”.

PLoS One. 2014 Apr 18;9(4):e95605. doi: 10.1371/journal.pone.0095605.

eCollection 2014.

2. Barat S¹, Bozko P¹, **Chen X**¹, Scholta T¹, Hanert F¹, Götze J¹, Malek NP¹, Wilkens L², Plentz RR¹

“Targeting c-MET by LY2801653 for treatment of cholangiocarcinoma”.

Molecular carcinogenesis (manuscript in revision)

10. Acknowledgments

I would like express my immense gratitude to Prof. Dr. med. Ruben R. Plentz for giving me the opportunity to work on this project and for supervising me as well as his continuous encouragement to keep up my spirit. Thanks to Prof. Dr. med. Nisar P. Malek for his great discussion of the projects during our lab meetings.

I am very grateful to Prof. Dr. med. Bence Sipos and Prof. Dr. med. Markus Kalesse for sharing their knowledge for my thesis.

Biggest thanks to Samarpita Barat who has been a wonderful friend, colleague and advisor. I am very grateful to Bui Khac Cuong for all the help he offered during my period in the lab.

Special thanks to Dr. rer. nat. Chih-Jen Hsieh and Jing, Lu for their great and continuous support in both professional and personal life. Thanks to Przemyslaw Bozko for his critical discussion and guidance in research reports. Hilde keppler thanks a ton for making the life in lab very lively and you willingness to help endlessly. Many thanks to Alena, Julian, Mathias, Tim, Franzi, Annika, Bhariya for their supports.

My special thanks to my parents in China and my friends in Tübingen (Leilei, Dongyun, Yiwen, Huiying, Jiajia, Ye, Chao, Xinyao, Layou, Xiaomin, Yi....) for supporting and their encouragement in whatever I am doing. I love you all.

Xi, Chen
Tübingen, 2015

11. Curriculum Vitae

Xi Chen

Personal Information

Date of Birth: 10.11.1983

Place of Birth: Shanghai, China

Nationality: Chinese

Email: xchen1110@hotmail.com or superrise@hotmail.com

Tel: +491636738793; +8613817096381

Educaiton

DOCTORAL STUDY (2013-2016): Universitätsklinikum Tübingen,
Internal Medicine I, Tübingen, Germany

Doctor of Medicine, Major in Internal Medicine/Gastroenterology

POSTGRADUATE (2007-2009): school of medicine, Shanghai
Jiao Tong University, China

Master of Medicine, Major in Internal Medicine/Gastroenterology

UNDERGRADUATE (2002-2007): school of medicine, Shanghai
Jiao Tong University, China

Bachelor of Medicine, Major in Clinical Medicine

Research Experience:

MD: Since October 2013

Universitätsklinikum Tübingen, Tübingen, Department of Internal Medicine I (Gastroenterology, Hepatology and Infectious diseases)

Project Handling:

1. Argyrin F therapy attenuates carcinogenesis of pancreatic adenocarcinoma (PDAC).
2. Jak2 inhibitor (INCB018424) impairs carcinogenesis of pancreatic adenocarcinoma (PDAC) via JAK-STAT pathway *in vitro* and *in vivo*.

Master's Thesis: Oct 2007-Jun 2009

1. School of Medicine, Shanghai Jiao Tong University, Shanghai, China.
 2. Ruijin Hospital, Department of Gastroenterology
- Thesis title: "Role of Classification of Pancreatic Cancer: Comparison of Japanese and UICC Classifications".

Conference Experience and poster presentations

Chen X, Barat S, Bozoko P, Sipos B, Kalesse M, Malek NP, Plentz RR.

"Argyirin F therapy attenuates carcinogenesis of pancreatic adenocarcinoma (PDAC)". Poster presentation 47th annual meeting of the European Pancreatic Club (EPC), Toledo, Spain, June 2015.

Chen X, Barat S, Bozoko P, Sipos B, Kalesse M, Malek NP, Plentz RR.

“Argyirin F therapy attenuates carcinogenesis of pancreatic adenocarcinoma (PDAC)”. Oral presentation in Deutsche Gesellschaft für Gastroenterologie, Verdauungs- und Stoffwechselkrankheiten (DGVS), Leipzig, Germany, September 2015.

Chen X, Barat S, Bozoko P, Sipos B, Kalesse M, Malek NP, Plentz RR.

“Argyirin F therapy attenuates carcinogenesis of pancreatic adenocarcinoma (PDAC)”. Oral presentation in German Cancer Congress (DKK), Berlin, Germany, February 2016

Chen X, Barat S, Bozoko P, Sipos B, Kalesse M, Malek NP, Plentz RR.

“Treatment of pancreatic ductal adenocarcinoma (PDAC) by argyirin F (AF) + gemcitabine (G)”. Poster presentation, GI ASCO San Francisco, USA, January 2016.

Research Skill

- Basic experimental skills;
- Molecular biological skills: Real-time PCR, Western blotting, Northern blotting, Southern blotting, Elisa, immunohistochemistry, DNA, RNA and Protein extraction and purification;
- Cell biology: quantitative image analysis (using microscope and inverted microscope), cell collection;

Language and skills

College English Test-Band Six. Skilled in reading, listening, writing and translation.

Proficiency with Windows, Microsoft Office, SPSS, Graphpad Prism and FlowJo.